Master's thesis

NTNU
Norwegian University of Science and Technology
Faculty of Natural Sciences
Department of Chemical Engineering

Kristine Maria Nettum

Simulation Study and Economical Analysis of Absorption Alternatives for Biogas Upgrading

Master's thesis in Chemical Engineering and Biotechnology
Supervisor: Hanna Knuutila
June 2019

NTNU
Norwegian University of
Science and Technology

Kristine Maria Nettum

Simulation Study and Economical Analysis of Absorption Alternatives for Biogas Upgrading

Master's thesis in Chemical Engineering and Biotechnology
Supervisor: Hanna Knuutila
June 2019

Norwegian University of Science and Technology
Faculty of Natural Sciences
Department of Chemical Engineering

NTNU
Norwegian University of
Science and Technology

Preface

This thesis was written during the spring semester of 2019 as the final part of my master's degree at the Department of Chemical Engineering at the Norwegian University of Science and Technology.

I would like to thank everyone in the environmental and reactor engineering group for help throughout the entire semester, and I would especially like to thank Professor Hanna Knuutila and PhD Candidate Ricardo Ramos Wanderley for incredible guidance and support.

I would also like to thank all my friends in Trondheim making these last five years some of the most memorable years in my life so far.

Trondheim June 10, 2019

Kristine Maria Nettum

Abstract

Biogas is an important renewable energy source and one of the largest problems during production is the price of biogas upgrading. This makes the research into different methods for biogas upgrading important. This study intends to draw a fair comparison of three different methods for biogas upgrading, water-scrubbing, organic solvent scrubbing using DEPG (dimethyl ether of polyethylene glycol) and amine scrubbing using MEA (monoethanolamine). Simulations are carried out in Aspen Plus v. 10.1, where an upgrading plant of each technology is designed and optimized. This modelling part is followed by an investment analysis. Results for each case are then compared.

In the simulations, targets of a 97.5% pure biomethane stream and a maximum of 5% methane slip are met with all technologies. In addition, recovery of a pure CO_2 stream is preferred, so that CCS (carbon capture and storage) alternatives can be implemented. Both the biomethane and CO_2 stream is compressed to 80 bars so that the delivery streams can be compared on a equal basis. The NRTL-RK thermodynamic model is used for the water-scrubbing and MEA-scrubbing, whereas the PC-SAFT model is used for the DEPG-scrubbing. A VLE (vapour-liquid equilibrium) validation is done for each solvent, checking that the models accurately predict experimental data from literature.

Overall, the results show that the energy consumption decreases in the order of water-scrubbing > DEPG-scrubbing > MEA-scrubbing, and the methane loss is at maximum value for the physical solvent cases while it is really low for the chemical absorption case. The overall energy consumption is calculated in terms of heat by using a electricity-to-heat approximation factor equal to the efficiency of a gas turbine. In water-scrubbing the main contributor to the energy penalty is the reboiler duty of around 9.0 MJ/kg CO_2 removed and a total energy consumption of around 13.0 MJ/kg CO_2 removed at an optimized L/G-ratio of 143. The MEA-scrubbing case has a reboiler duty of around 3.8 MJ/kg CO_2 removed and a total consumption of around 6.3 MJ/kg CO_2 removed at a optimized L/G-ratio of 9.5. In the DEPG-scrubbing case nitrogen stripping is used to avoid high reboiler temperatures. This decreases the energy duties and the total energy requirement is found to be 6.8 MJ/kg CO_2 removed at a optimized L/G-ratio of 100. The chemical absorption process has a lower energy requirement, and the methane slip is by far the lowest. The CO_2 stream is also purest for this process as there is no stripping gas contamination or high portions of methane due to methane slip.

Payback time is lower for the MEA-scrubbing case, this is clear in the investment analysis. The MEA case has the highest IRR (internal rate of return) of 3.1% while the water-scrubbing and DEPG-scrubbing have an IRR of 1.5% and 1.1% respectively. A sensitivity analysis is also performed, showing that the MEA case is also more robust against changes in methane, CO_2

and biogas prices as well as changes in the investment cost.

It is concluded that the MEA-scrubbing case is the most competitive process for reaching the desired specifications, due to lower methane slip which increases income and lowers emissions. It is also concluded that further optimization of the MEA-scrubbing process could give even better result for this case. Redesign of the water-scrubbing case with the use of stripping gas and a flash for recirculating of methane might improve this case considerably, and this should also be looked into in the future.

Sammendrag

Biogass er en viktig fornybar energikilde. Ett av de største problemene ved produksjon av biogass er prisen for biogass oppgradering, dette gjør forskning på forskjellige oppgraderingsmetoder viktig for å gjøre en fornybar energikilde mer lønnsom. Intensjonen med denne oppgaven er å lage en rettferdig sammenligning mellom tre forskjellige metoder for biogass oppgradering, vann-skrubbing, organisk løsemiddel-skrubbing ved bruk av DEPG (dimetyl eter av polyetylen glykol) og amin-skrubbing ved bruk av MEA (monoetanolamin). Simuleringene ble gjort i Aspen Plus versjon 10.1. Her ble ett anlegg fra hver teknologi designet og optimalisert. Etter simuleringene ble det utført en investeringsanalyse. Resultatene fra hvert anlegg ble til slutt sammenlignet.

I simuleringene ble mål om en 97,5% ren biometan strøm og et maksimum på 5% metantap oppfylt for alle teknologiene. I tillegg er det foretrukket å få en så ren CO_2 strøm som mulig, sånn at CCS (karbonfangst og lagring) kan implementeres. Både biometan og CO_2 strømmene blir komprimert til 80 bar sånn at produktstrømmene kan sammenlignes på samme basis. For vann-skrubbing og MEA-skrubbing simuleringene ble den termodynamiske modellen NRTL-RK brukt mens for DEPG-skrubbing ble PC-SAFT modellen brukt. En VLE (gass-væske likevekt) validering er utført for hvert løsemiddel for å se at modellene korresponderer bra med data fra litteraturen.

Energiforbruket synker i følgende rekkefølge: vann-skrubbing > DEPG-skrubbing > MEA-skrubbing. Metantapet er på maksimum verdi for prosessene med fysisk absorpsjon mens verdien er veldig lav for kjemisk absorpsjon. Det totale energiforbruket er beregnet som varme, og dette er gjort ved hjelp av en elektrisitet-til-varme approksimasjon lik effektiviteten til en gassturbin. I vann-skrubbing er hovedbidragsyteren til energiforbruket reboileren som bruker rundt 9,0 MJ/kg CO_2 fjernet, prosessen har ett totale forbruk på rundt 13,0 MJ/kg CO_2 fjernet med en optimalisert L/G-rate på 143. Reboileren i MEA-skrubbing prosessen bruker rundt 3,8 MJ/kg CO_2 fjernet og har ett totalt energiforbruk på 6,3 MJ/kg CO_2 fjernet, dette er med en optimalisert L/G-rate på 9,5. DEPG-skrubbing prosessen ble designet litt annerledes enn de andre to prosessene, reboileren ble erstattet med nitrogen som strippe-gass på grunn av veldig høye temperaturer i reboileren. Dette senker energiforbruket og det totale energiforbruket ble på rundt 6,8 MJ/kg CO_2 fjernet på en optimalisert L/G-rate på 100. Dette viser at den prosessen med lavest energiforbruk og lavest metantap er MEA-skrubbing. CO_2 strømmen er også renest med denne prosessen siden det ikke er noe strippegass eller høye verdier av metan på grunn av metantap.

Tilbakebetalingstiden er lavere for MEA-skrubbing prosessen enn for de andre to, dette kommer klart frem av investeringsanalysen. MEA prosessen har høyest IRR (intern avkastning) på 3,1% mens vann-skrubbing og DEPG-skrubbing har henholdsvis 1,5% og 1,1%. En sensi-

tivitetsanalyse ble også gjort, den viser at MEA prosessen er også den prosessen som er mest robust mot endringer i metan, CO_2 og biogass pris, i tillegg til endringer i investeringskostnadene.

Det er konkludert med at MEA-skrubbing er den mest lovende prosessen for å nå de satte spesifikasjonene. Dette er på grunn av lavt metantap noe som øker inntektene og senker utslipp. Det er også konkludert med at MEA prosessen må videre optimaliseres noe som kan gi enda bedre resultater. Redesign av vann-skrubbing prosessen hvor rebileren er byttet ut med strippegass for å senke energikostnadene, og resirkulering av metan er implementert for å senke metantapet kan kanskje forbedre denne prosessen. Dette er viktig å se på fremover.

Contents

List of Figures

List of Tables

Abbreviations

Abbreviation	Explanation
CCS	Carbon Capture and Storage
C_3H_8	Propane
CH_4	Methane
CO_2	Carbon dioxide
DEPG	Dimethyl ether of polyethylene glycol
GHG	Greenhouse gases
H_2	Hydrogen
H_2O	Water
H_2S	Hydrogen sulfide
IRR	Internal rate of return
LCV	Lower calorific value
MEA	Monoethanolamine
N_2	Nitrogen
N_2O	Dinitrogenoxide
NH_3	Ammonia
NRTL-RK	Non random two liquid molel
NTNU	Norwegian University of Science and Technology
PC-SAFT	Perturbed-chain statistical associating fluid theory
ROI	Return on investment
STP	Standard temperature and pressure
VFA	Volatile fatty acid
VLE	Vapour liquid equilibrium

1 Introduction

1.1 Background and Motivation

Below the motivation of this thesis is given, including reflections about global warming and renewable energy. Furthermore, a short introduction to biogas production and upgrading is provided.

1.1.1 Global Warming

The earth's atmosphere is a protecting layer of gas that regulates the temperature on earth. When radiation waves from the sun hit the planet's atmosphere, some of the radiation is reflected back into space and some passes through, hitting the earth's surface. Some of this radiation is absorbed by land and ocean, heating them up, and some is reflected back towards space. Some of this heat that radiated back towards space is trapped by gas-molecules in the atmosphere, and this keeps the planet warm enough to sustain life. This is called the greenhouse effect. There are multiple gases that have this ability to absorb the reflecting radiation, and they are called greenhouse gases. Examples of greenhouse gases are H_2O, CO_2, CH_4 and N_2O. [1]

Anthropogenic greenhouse gas emissions have increased since the preindustrial era. This is mainly due to burning of coal and other fossil fuels, driven by economic and population growth [2]. This has resulted in higher concentration of the greenhouse gases in the atmosphere, leading to a warmer climate on earth. This extra heating of the planet is called global warming. As opposed to the impression of many sceptics, there is a scientific consensus that the rapid change in climate that we see today is man made and due to the burning of fossil fuels [3]. Some of the consequences of this change are more extreme weather events, reduced agricultural production, ocean acidification, loss of biodiversity and less availability of freshwater [2].

Of all the greenhouse gases, CO_2 is the one that receives more attention. This is because the CO_2 emissions from combustion of fossil fuels and industrial processes are the biggest contributor to the global GHG emissions with 62% in 2010 [2]. Continuous research into decreasing CO_2 emissions have been a priority for many years now, and is still a priority today. Many possible solutions to reducing the emissions are suggested, some which are:

- Increasing the energy efficiency of processes by help of new technologies.
- Carbon capture and storage (CCS)

- Changing fuels in the transport industry to fuels with lower carbon release.
- Changing electricity source from CO_2 emitting sources to non-CO_2 emitting sources like solar power and wind power.

Of all these alternatives, it is assumed that CCS is going to be the the most important alternative in a short timespan. CCS is recognised as a key technology for reducing the greenhouse gas emissions around the world [4]. The use of fossil fuels can not stop immediately as there is no alternative fuels that can provide the world's energy demand as of today. This means that processes that can capture CO_2 and keep it from the atmosphere are very interesting. CCS technology consists of three major steps: (i) capturing the CO_2 from large industrial processes like coal and natural-gas-fired power plants, steel mills, cement plants and refineries, (ii) compressing and transporting the gas to the storage site, and (iii) injection of the gas into rock formations deep in the ground. [4]

1.1.2 Renewable Energy

It is predicted that the energy demand in the world will grow in the years to come. This is mainly due to economical growth in many countries, especially in Asia [5]. A prediction of the increase in production of different energy sources is given in figure 1.1.1. The production of renewable energy sources is predicted to increase a lot by 2040, indicating that research into different renewable energy sources is incredibly important.

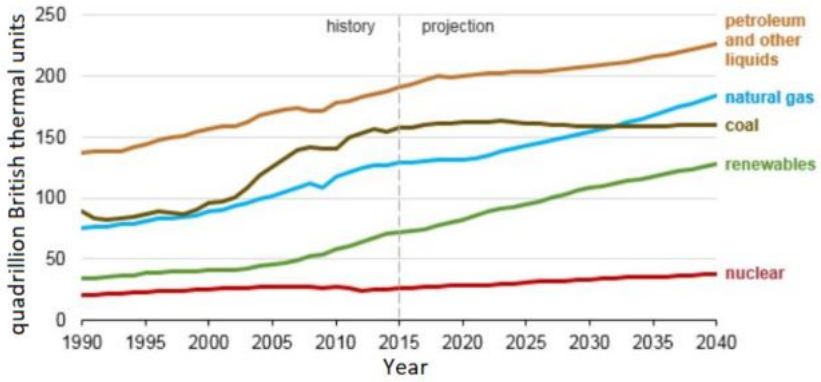

Figure 1.1.1: World energy production by source, figure borrowed from [5].

Renewable energy sources of limitless duration and smaller environmental impact such a wind-power, solar-power, hydro-power and biogas are important when the world is facing increasing energy demands and pollution issues [6]. Rising GHG emissions and the fact that the fossil fuel sources are running out makes it incredibly important to research into renewable energy sources.

Biogas-production is a well established, sustainable process for generation of renewable

energy and simultaneous treating of organic waste [7]. Advantages of biogas as an energy source is that is has no geographical limitations and the technology is well known [6]. With this, biogas will probably be an important energy source in the future.

1.1.3 Biogas

As mentioned before, biogas is a renewable energy source. It can be used for heating, combined heat and power generation, as transportation fuel and it can substitute for natural gas, which has diverse applications. The two latter examples demand that biogas is upgraded to biomethane, which means removing the CO_2 from the gas. This process is called biogas upgrading. [8]

The production of biogas is done through an anaerobic digestion which is split into four smaller processes [7]. These processes are shown in figure 1.1.2. First, complex organic matter is processed into simpler monomers through hydrolysis. Next, the monomers go through a fermentation process by acidogenic bacteria called acidogenesis. This is where the monomers are transformed into intermediate products consisting of CO_2, H_2, alcohols and low molecular weight volatile fatty acids (VFAs). In the third step the alcohols and the VFAs are oxidized by hydrogen-producing acetogenic bacteria into acetate. This process is called acetogenesis. Finally, the acetate, H_2 and CO_2 are transformed into a mixture of CH_4 and CO_2 through acetotropic and hydrogenotrophic methanogenesis. [8]

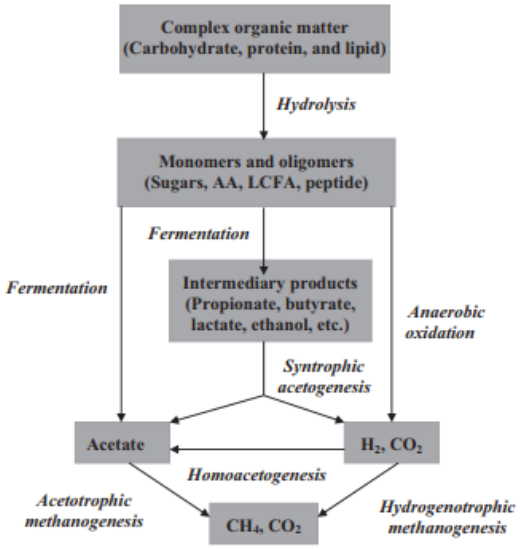

Figure 1.1.2: Biogas production, figure borrowed from [8]

Biogas consists mainly of CH_4 in a range of 50-70%vol/vol and CO_2 in a range of 30-50%vol/vol. The ratio between these two components vary with the feedstock and the operating conditions of the process. Biogas also contains other trace components, like N_2 (0-3% vol/vol), H_2O (5-10% vol/vol), O_2 (0-1%vol/vol), H_2S (0-10000ppmv), NH_3 (0-200 mg/m^3) and siloxanes (0-41 mg/m^3). [7]

1.1.4 Biogas Upgrading

Due to increasing interest in using biogas as a substitute for natural gas and as transportation fuel, biogas upgrading is getting increasingly important. Apart from the methane, all components in the gas are considered impurities. Methane is the energy carrier in the gas, and the energy content is measured in Lower Calorific Value (LCV) (MJ/$m^3(CH_4)$). The higher the concentration of methane, the higher the energy content. Biogas upgrading concentrates on the removal of CO_2 from the biogas. Other impurities in the gas are removed before the biogas upgrading in a process called biogas cleaning. This process is executed regardless of if the upgrading will take place or not, and is done because some of these components are corrosive and will damage the equipment in downstream processes. [7] The target for the purity of methane varies for different industries and between countries. The strictest targets are for the biomethane that will be injected into the natural gas grid, and for example in Sweden this target is 97 ± 1 mole% methane content. [9] Requirements for other countries are given in [9] and [10].

Many technologies exist for the removal of CO_2 from biogas, among them physical absorption using water or organic solvent and chemical absorption using a amine solvent [7]. These methods are discussed later.

1.2 Objective

The production of biomethane is typically divided into three parts. First (i) the production of biogas containing mainly CH_4 and CO_2, second (ii) the biogas cleaning and upgrading where CO_2 and other impurities are removed from the biogas, producing biomethane, and last (iii) the liquefaction or pressurization of the gas for transport. Since a big obstacle for implementation of sustainable biogas energy systems is the cost of the biogas upgrading, this is an important area for research.

The objective of this work is to achieve a fair comparison of three different methods for biogas upgrading, water-scrubbing, organic solvent scrubbing using DEPG and amine scrubbing using MEA with focus on energy consumption and cost. The overall objective can be divided into the following sub-objectives:

- Simulate three different methods for biogas upgrading using Aspen Plus software, version 10.1.
- Execute a investment analysis of each plant.
- Compare the energy demand from the simulations and the investment analysis to see which plant is more promising.

- Evaluate the environmental aspects of the plant.

All three processes have the same starting point, with values given in table 1.2.1. The size of the biogas stream was set to 500 m^3/h after the average size of Danish biogas plants [11] [12]. The methane gas is purified to the same purity in each case, 97.5% (mol/mol) after Swedish standards [9] [10], and the methane slip has an upper limit of 5% mol/mol. The product streams are both pressurized to 80 bars. The pressure at which the gas is compressed when it is pumped into the gas grid, or pumped under ground for CCS is above the pressure, and 80 bars is chosen to get a fair comparison between the processes that will be investigated. It is also attempted to get as clean a CO_2 stream as possible, to be able to apply CCS technology.

Table 1.2.1: Data for the raw biogas.

Temperature [°C]	30
Pressure [bar]	1
Volume flow [m^3/h]	500
Mass flow [kg/h]	575
CH_4 fraction (%mol/mol) (dry)	60
CO_2 fraction (%mol/mol) (dry)	40

1.3 Outline

Chapter 1 contains the background and motivation of the processes as well as the objective of the thesis. Chapter 2 gives a description of the biogas upgrading technologies that are simulated in this thesis, this includes process descriptions and advantages and disadvantages with each method. Chapter 3 describes the simulations models that are used, including the VLE validation. The simulation results are presented and discussed in chapter 4 including complete simulations flowsheets, important parameters from the simulations and the final results. The results of the economic analysis are given in chapter 5, including the cost of equipment, an investment analysis and sensitivity analysis of the plants. The different cases are compared both in regards of simulation performance and economic analysis in chapter 6. Chapter 7 gives suggestions to further work while chapter 8 gives the conclusions of this thesis.

2 Biogas Upgrading Technologies

The removal of CO_2 from biogas is mainly performed by physical/chemical technologies due to the commercial availability and the fact that the technologies have been around for a long time [9]. These technologies are divided into scrubbing-technologies with different solvents; (i) water, (ii) organic solvents or (iii) chemical solvents, in addition to (iv) pressure swing adsorption and (v) cryogenic CO_2 separation. This work focus on the scrubbing technologies, which are all described below.

2.1 Water-scrubbing

The water-scrubbing technology is the most common way to upgrade biogas today. This is a physical absorption technology using water as the absorbent. The water can absorb both CO_2 and H_2S and the process relies on the fact that CO_2 is 26 times more soluble in water at 25 °C than methane [7].

Figure 2.1.1 shows the flowsheet of the water-scrubbing process. The biogas is pressurized to 6-20 bars and sent in to the absorption column at the bottom. Water flows counter currently downwards in the column [13]. The column is filled with packing to increase the gas-liquid contact surface. The water containing CO_2 leaves at the bottom of the column, while the clean upgraded biogas leaves at the top. The CO_2 rich water is decompressed first to around 2-3 bars in a flash drum, to recover any trace CH_4 that have dissolved in the water. Then water is regenerated in a desorber column, where CO_2 is stripped from the water using air as stripping-gas at atmospheric pressure [7]. After a drying step the product can reach a 99% purity.

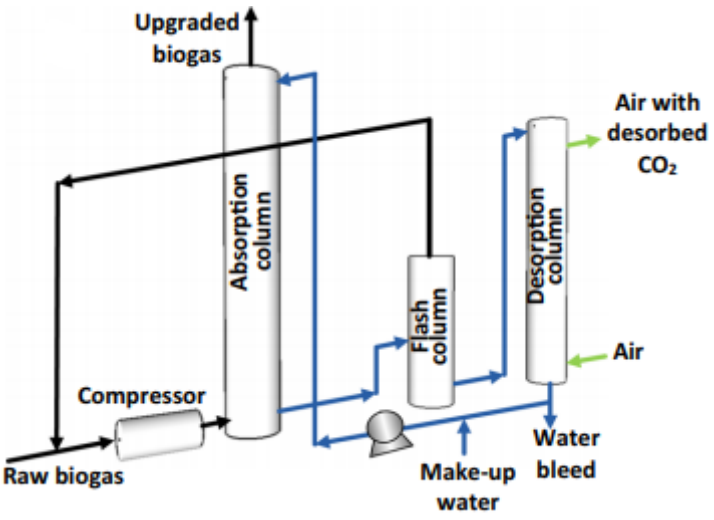

Figure 2.1.1: Generic flowsheet of the water-scrubbing process [9].

Advantages with water-scrubbing are that it is not sensitive to impurities, so pre-cleaning is not strictly required. It is also simple in operation. Disadvantages are that large amounts of water are needed, meaning large equipment sizes in addition to the cost of pumping the large solvent stream through regeneration [14]. Another disadvantage of the water-scrubbing process is the fact that air is used as stripping gas. This leads to a mixed byproduct-stream, not a clean CO_2 stream. The CO_2 can not be stored, as the separation of CO_2 from the air is very expensive. This means CCS is not an option.

Water scrubbing without regeneration of the water is also a possibility, but not better in a environmental aspect as the CO_2 is still not captured. Another alternative is to use steam as the stripping gas, by installing a reboiler in the desorber column, regenerating the water using heat. As the objective of this thesis is to compare different processes with the capture of CO_2 being a important factor, this is the process that is further discussed.

2.2 Organic Solvent Scrubbing

Organic solvent scrubbing is another physical absorption method and the principal is similar to that of the water-scrubbing case. Instead of water the solvent used is an organic liquid such as methanol or dimethyl ethers of polyethylene glycol (DEPG) [14]. Trade-names for this latter solvent is Selexol and Genosorb [10]. The removal of CO_2 is based on the same principle as for water-scrubbing, a difference in solubility between CO_2 and CH_4.

Figure 2.2.1 shows the flowsheet of the organic solvent-scrubbing process. The biogas is dried and compressed and enters the absorber column at the bottom at a pressure of 6-10 bars and a temperature of 20 °C. The organic solvent solution flows counter-currently downwards in the column. The clean gas exits at the top of the column. The liquid exits at the bottom and is heated in a process heat exchanger before it enters a flash tank, where the pressure is released to separate methane that is recirculated back to the biogas stream to avoid methane loss. The liquid leaving the flash is further heated before it enters the desorber, where the solvent is regenerated using a stripping gas at atmospheric pressure and a temperature of around 80 °C [15]. The solvent enters at the top and the stripping gas flows counter-currently upwards. The regenerated liquid exits at the bottom of the desorber, where it is pumped back up to the absorber pressure and cooled back down to 20 °C before it reenters the absorber. CO_2 leaves the desorber together with the stripping gas at the top of the desorber [9].

Advantages for the organic scrubbing is that CO_2 is 5 times more soluble in DEPG than in water, which means that the liquid flow needed for removing the same amount of CO_2 is lower, meaning smaller equipment and thereby lower cost [9] [10]. The solvent also has a low vapour pressure, meaning that the loss of DEPG is very low [13]

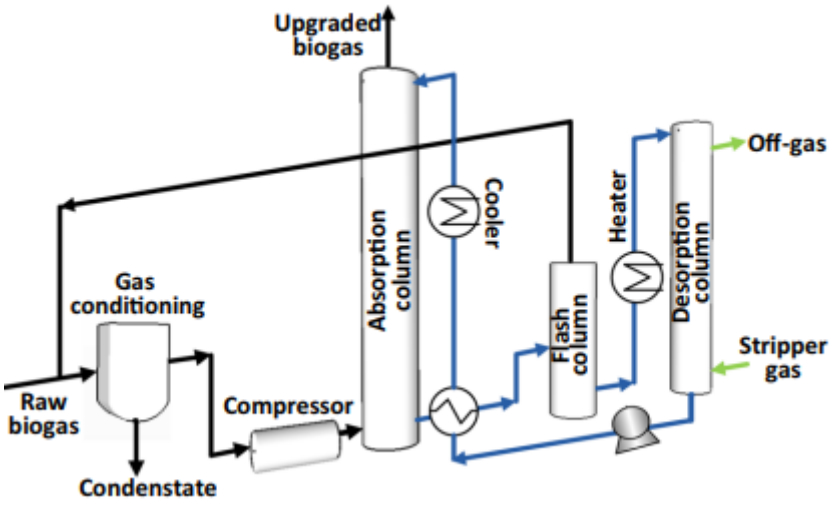

Figure 2.2.1: Generic flowsheet of the organic solvent scrubbing process [9].

Environmental concerns are also present here as in water-scrubbing in regards of the stripping gas leading to a CO_2 stream that is not pure. Regeneration using heat could also be an alternative here, but the DEPG is much less volatile than water, and the heat requirement could be very high.

2.3 Amine Scrubbing using MEA

While the other methods rely on increased physical solubility of CO_2 in a solvent, chemical absorption additionally rely on chemical reactions between the solvent and the solute. These reactions increase the solubility of the gases enormously compared to just physical absorption. There are some properties that characterize a good solvent: (i) High capacity for absorbing CO_2 (high maximum loading and high selectivity), (ii) low regeneration energy (low enthalpy of absorption), (iii) high stability, (iv) high sensitivity for equilibrium temperature and (v) wide possibility of operating conditions [16].

Monoethanolamine (MEA) is a primary amine with a reactive nitrogen group, as can be seen in figure 2.3.1. MEA, developed over 80 years ago, is the most common solvent used for post-combustion chemical absorption of CO_2 [17]. The typical reactions involved during chemisorption of CO_2 into MEA are given in table 2.3.1.

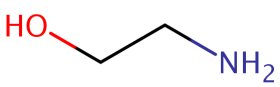

Figure 2.3.1: MEA molecule structure.

A important reaction is reaction 6 which describes how CO_2 is absorbed by MEA, which

Table 2.3.1: The chemical reactions for chemical absorption using MEA.

Reaction	Number
$MEAH^+ + H_2O \longleftrightarrow MEA + H_3O^+$	1
$2H_2O \longleftrightarrow H_3O^+ + OH^-$	2
$OH^- + CO_2 \longrightarrow HCO_3^-$	3
$HCO_3^- + H_2O \longleftrightarrow CO_3^{2-} + H_3O^+$	4
$HCO_3^- \longrightarrow OH^- + CO_2$	5
$MEA + CO_2 + H_2O \longrightarrow MEACOO^- + H_3O^+$	6
$MEACOO^- + H_3O^+ \longrightarrow MEA + CO_2 + H_2O$	7

happens in the absorber. MEA and CO_2 form carbamate. Reaction 7 is the reverse of reaction 6, and is what happens in the desorber. As reaction 6 is exothermic, it is favorable to have a low temperature in the absorber, and a high temperature in the desorber. The protonation of MEA is described with reaction 1, and reaction 2 is the standard water-dissociation reaction. Reactions 3 and 4 give the first and second dissociation of CO_2, and reaction 5 is the reverse of reaction 3.

Figure 2.3.2 shows the flowsheet of the chemical absorption process. The biogas enters the absorber at the bottom, at atmospheric pressure. The MEA solution flows counter-currently downwards in the column, and the CO_2 is absorbed into the solvent. The clean biomethane exits the top of the absorber while the rich-amine solution exits the bottom of the absorber. The liquid is heated in a cross heat exchanger before it enters the desorber column. The column is equipped with a reboiler, and vaporized solvent flows upwards in the column, as CO_2 desorbs from the liquid back into vapour-phase. The clean lean-solution is circulated back to the top of the absorber [13].

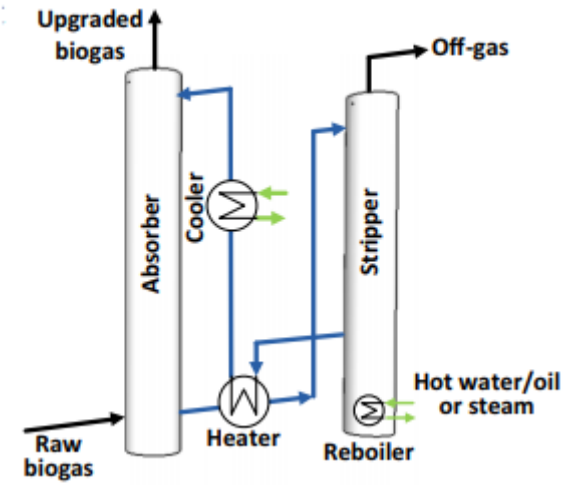

Figure 2.3.2: Generic flowsheet of the chemical solvent scrubbing process [9].

Advantages of this process are very high efficiency (very clean products) and very low methane loss [13]. MEA is popular due to the fact that is has the ability to totally remove acid gases at

low pressure. MEA also has other advantages, amongst them high capacity to absorb CO_2 due to low molecular weight and rapid reaction with CO_2. MEA is less volatile than many other amines and it also is relatively inexpensive [18].

One disadvantage is that MEA causes corrosion, which means that the MEA concentration in the solvent has to be kept low (20-30 wt%), again resulting in larger solvent streams, and thereby larger equipment and regeneration costs. Equipment costs also increase since the use of material like stainless steal is needed. Another disadvantage is the high heat of absorption for MEA, leading to a high heat requirement in the regeneration unit. Amines also volatilize over time, so injection of fresh amine will be needed [17].

3 Simulation Models

All simulations were carried out in Aspen Plus version 10.1. For the DEPG-scrubbing and MEA-scrubbing, an inbuilt template from Aspen was used as a base for the simulations. For water-scrubbing the model was made from scratch. A description of the models is given below.

The absorber and desorber columns for all three processes are simulated as rad-frac columns in Aspen Plus. A rate based model was used to calculate the CO_2 removal rates. Rate-based modelling approach is rigorous and offers higher model fidelity [19]. The model assumes separation happens between two phases due to mass-transfer, and equilibrium is achieved at the interface between the two phases. Maxwell-Stefan theory is used to calculate mass transfer rates. This is different from traditional equilibrium based modelling, where it is assumed that each theoretical stage consists of two well mixed phases that are in equilibrium with each other. This will always be an approximation since the two contacting phases will never be in equilibrium in a real column [19].

For choosing a model for water-scrubbing a literature study was done. It was found that multiple models were previously used. Some models that were mentioned were UNIQUAC, NRTL, NRTL-RK, UNIQ-RK, ELECNRTL and ENRTL-RK [20] [21]. All models were tested in Aspen Plus and compared with experimental data from literature [22] [23], which can be seen in figure 3.0.1. All models give good results for pressures below 10 bars. The UNIQUAC and NRTL models deviate from the experimental data at higher pressures, while the other models fit well with experimental data for the whole interval that was investigated.

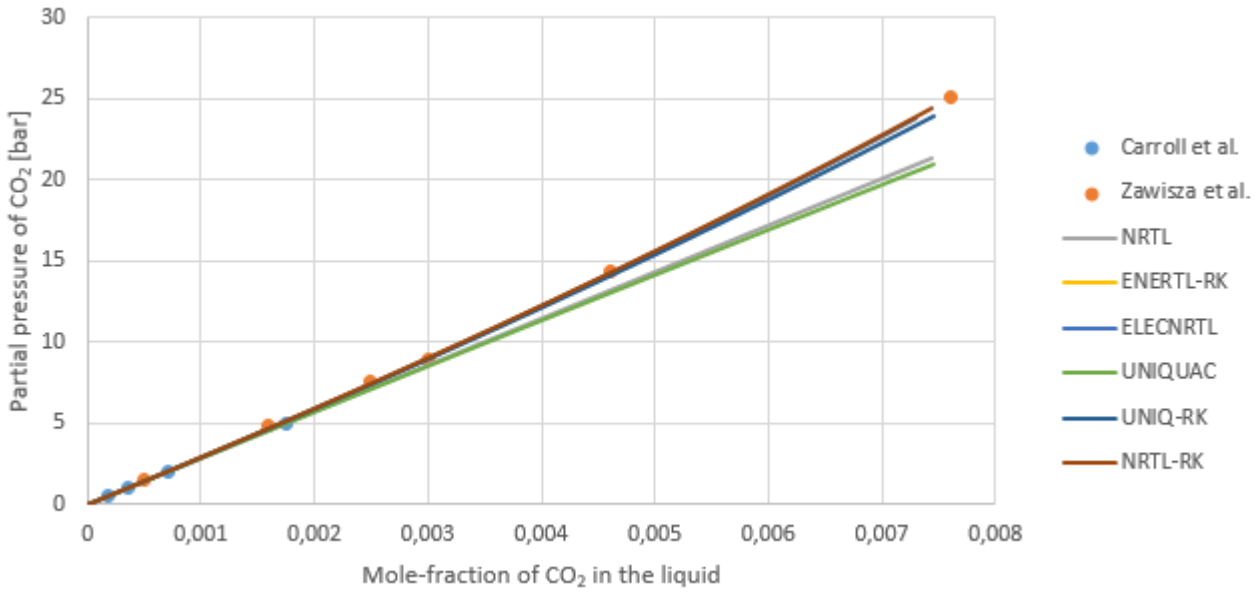

Figure 3.0.1: Tested models compared to literature data [22] [23].

Of the four models that fit well with the experimental data the NRTL-RK model was chosen because it was recommended in literature and also it is the same model that is used in the MEA-scrubbing template. This model uses a non-random two liquid model to calculate the activities, the basic assumption of this model being that the nonideal entropy of mixing is negligible compared to the heat of mixing. This is the case for electrolyte systems. The Redlich-Kwong equation of state is used to describe the vapour phase [24].

A template called "Aspen_Plus_DEPG_Model" was used as the basis for the DEPG-scrubbing simulations. This template uses the PC-SAFT (perturbed-chain statistical associating fluid theory) model.

A template called "NRTL-RK_Rate_based_MEA_Model" was used as the basis for the MEA-scrubbing simulations. This model is described above for the water-scrubbing case. The Kent-Eisenberg model is used to calculate the liquid mixture component fugacity coefficients and liquid enthalpy for the AMINES property method [24]. The chemical equations that are defined in Aspen Plus are given in table 3.0.1.

Table 3.0.1: The chemical reactions defined in Aspen Plus.

Reaction	Type	Number
$MEAH^+ + H_2O \longleftrightarrow MEA + H_3O^+$	Equilibrium	1
$2H_2O \longleftrightarrow H_3O^+ + OH^-$	Equilibrium	2
$OH^- + CO_2 \longrightarrow HCO_3^-$	Kinetic	3
$HCO_3^- + H_2O \longleftrightarrow CO_3^{2-} + H_3O^+$	Equilibrium	4
$HCO_3^- \longrightarrow OH^- + CO_2$	Kinetic	5
$MEA + CO_2 + H_2O \longrightarrow MEACOO^- + H_3O^+$	Kinetic	6
$MEACOO^- + H_3O^+ \longrightarrow MEA + CO_2 + H_2O$	Kinetic	7

3.1 VLE Validation

A vapour-liquid-equilibrium validation was performed for the models that would be used for each simulation to ensure that the models work as expected. Vapor-liquid equilibria was simulated in Aspen Plus and the simulated values were compared with literature data. This was done for the phase equilibrium between CO_2 and solvent, and between methane and solvent. The relative deviation between the simulation and the experimental data point were calculate using equation 3.1.1. Results from these validations can be seen below.

$$\text{Relative deviation} = \frac{\text{Experimental - Simulations}}{\text{Experimental}} * 100\% \tag{3.1.1}$$

3.1.1 Water-scrubbing

Figure 3.1.1 shows the VLE validation for the CO_2-H_2O system. The partial pressure of CO_2 is plotted as a function of the mole-fraction of CO_2 in the liquid phase together with a experimental data set for low pressures from 1-10 bars. Figure 3.1.2 shows the same for a experimental data set for pressures up to 70 bars. Figure 3.1.3 shows the VLE validation for the CH_4-H_2O system, the partial pressure of CH_4 plotted as a function of the mole-fraction of CH_4 in the liquid phase together with experimental data. Table 3.1.1 shows the calculated relative error for the mole-fraction between the simulations and the experimental data for all validations.

Table 3.1.1: Average relative error for the VLE-validation for the CO_2-H_2O system for high and low pressure and CH_4-H_2O system between the simulations and literature data [22] [25] [26].

CO_2-H_2O (0-10 bars)		CO_2-H_2O (1-70 bars)		CH_4-H_2O (10-80 bars)	
Temperature . [°C]	AR Error [%]	Temperature [°C]	AR Error [%]	Temperature [°C]	AR Error [%]
10	1.8	15	6.2	10	7.6
20	0.9	25	6.9	25	3.3
30	0.6	35	7.1	40	5.3
40	1.4	45	7.5		
50	2.3				
60	3.0				
70	3.9				

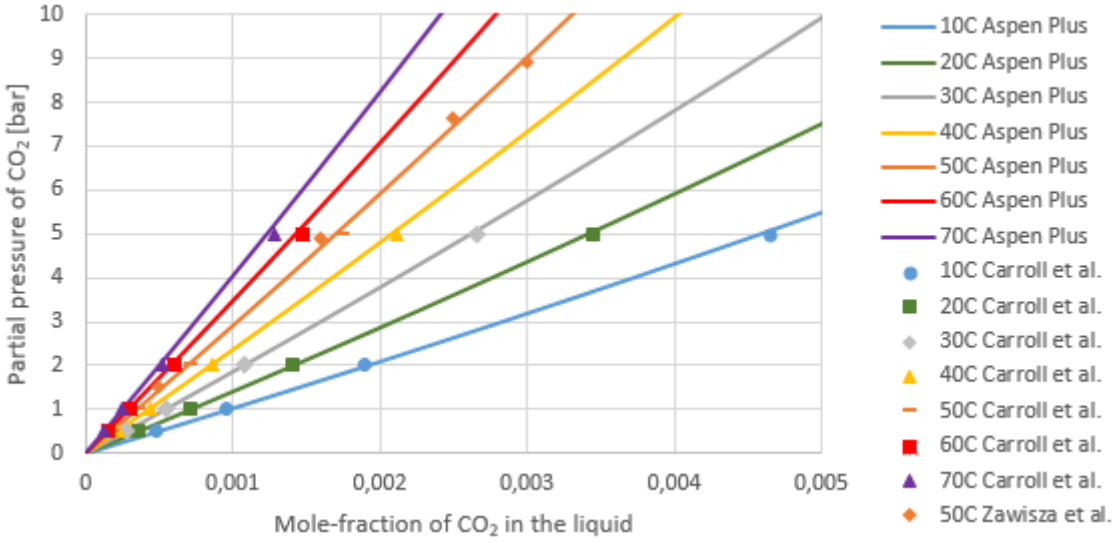

Figure 3.1.1: Aspen Plus simulation data and experimental data from literature [22] for the CO_2-H_2O system at low pressures.

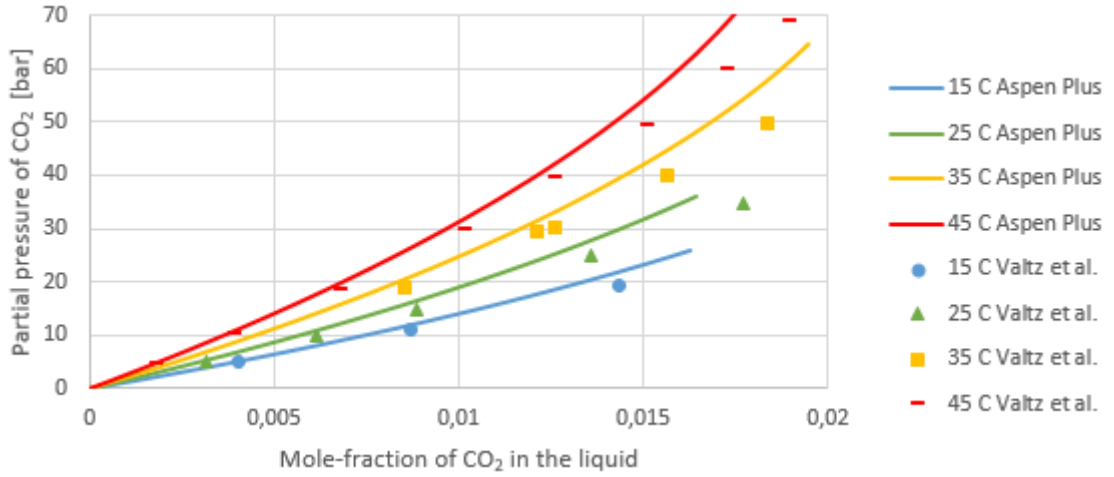

Figure 3.1.2: Aspen Plus simulation data and experimental data from literature [25] for the CO_2-H_2O system at high pressures.

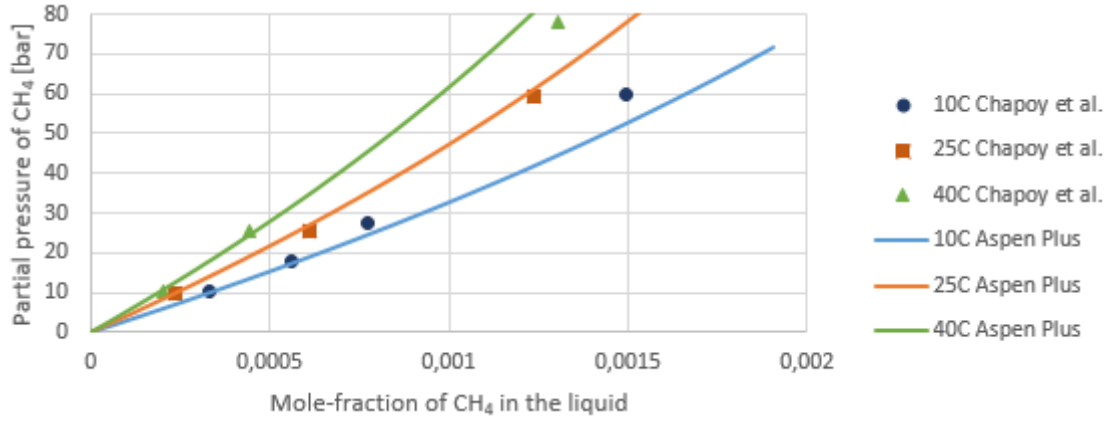

Figure 3.1.3: Aspen Plus simulation data and experimental data from literature [26] for the CH_4-H_2O system.

As can be seen from the relative errors the simulations seem to fit well with the experimental data for the water-scrubbing case, both in regards of CO_2 and methane. This especially applies within the operating pressure-range for the simulations (1-10 bars). This gives a good indication that the model works well within the desired interval.

3.1.2 Organic Solvent Scrubbing using DEPG

The VLE-validation for the CO_2-DEPG system can be seen in figure 3.1.4 and 3.1.5 where the partial pressure of CO_2 is plotted as a function of the mole-fraction of CO_2 in the liquid phase for two different data sets, one with pressures up to 40 bars and one with pressures up to 100 bars. Figure 3.1.6 shows the CH_4-DEPG system VLE validation. The partial pressure of CH_4 is plotted as a function of the mole-fraction of CH_4 in the liquid phase.The average relative error between the simulations and the data from literature are given in table 3.1.2.

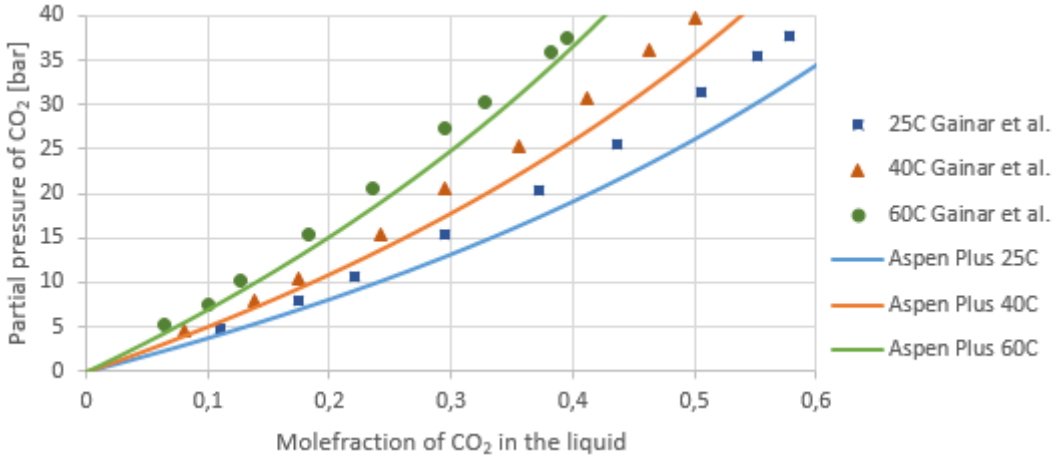

Figure 3.1.4: Aspen Plus simulation data and experimental data from literature [27] for the CO_2-$DEPG$ system at low pressures.

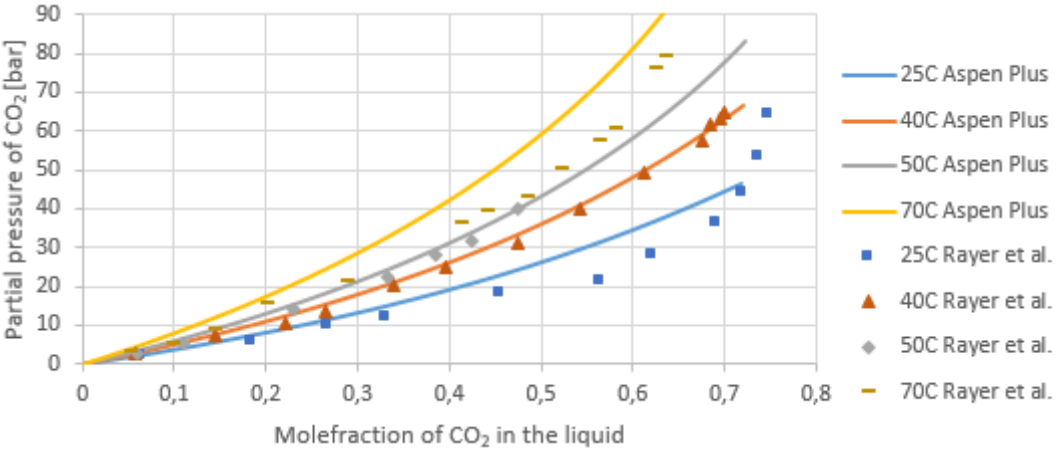

Figure 3.1.5: Aspen Plus simulation data and experimental data from literature [28] for the CO_2-$DEPG$ system at high pressures.

Table 3.1.2: Average relative error for the VLE-validation between simulations and literature data for the CO_2-DEPG system at high and low pressure, and for the CH_4-DEPG system [27] [28] [29]

CO_2-DEPG (5-40 bars)		CO_2-DEPG (1-80 bars)		CH_4-DEPG (0-40 bars)	
Temperature	AR error	Temperature	AR error	Temperature	AR error
25	11.8	25	12.6	25	38.6
40	9.1	40	3.7	40	58.4
60	8.2	50	8.5	60	71.2
		70	15.3		

For the CO_2-DEPG validation the simulations fit well with the experimental data, both at high and low pressures and for all temperatures. The model seems to fit best at temperatures around 40°C. For the CH_4-DEPG system the validation does not give as good results. As

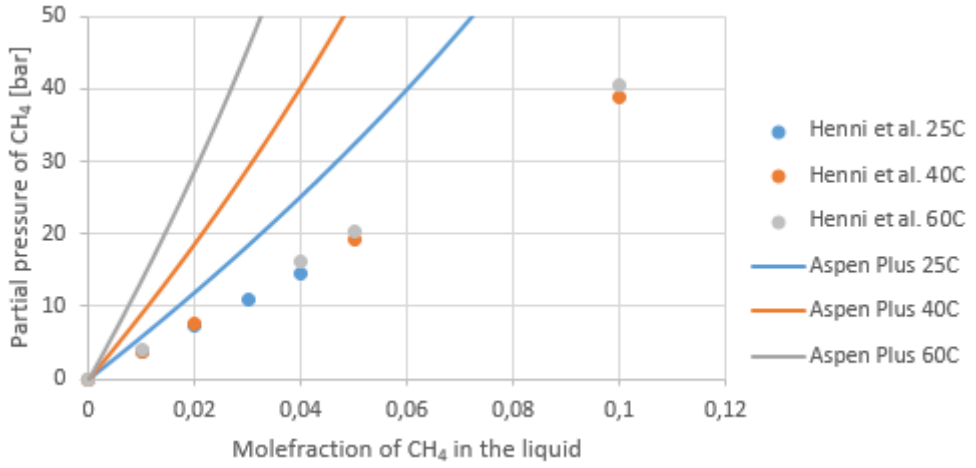

Figure 3.1.6: Aspen Plus simulation data and experimental data from literature [29] for the CH_4-$DEPG$ system.

can be seen in the figure and by the relative errors the model persistently underestimate the methane slip in the process, as it predicts less solubility of CH_4 in DEPG than what is actually seen in experimental data. The CH_4 solubility is anyway low compared to CO_2 solubility (at 40°C and 10 bars the molefraction in the liquid is about 0.03 and 0.18 respectively) and relevant only for the estimations of the methane slip. Therefore, it was decided to use the Aspen Plus template as it is and correct the simulated methane loss values manually after the simulations instead of building a new model from scratch.

3.1.3 Amine Scrubbing using MEA

The VLE-validation for the amine scrubbing case can be seen in figure 3.1.7 where the partial pressure of CO_2 is plotted against the loading of CO_2 in the liquid phase. The average relative errors for the loading of CO_2 can be seen in table 3.1.3. The validation for the CH_4-MEA-H_2O case was not executed as the system was assumed to be similar to the CH_4-H_2O case, which uses the same model equation and is validated above for the water-scrubbing case.

Table 3.1.3: Average relative error for the VLE-validation between simulations and literature data [30] [31] for the CO_2-MEA-H_2O system.

Temperature [C]	Average relative error [%]
40	5.76
60	5.40
80	11.31
100	8.33
120	6.04

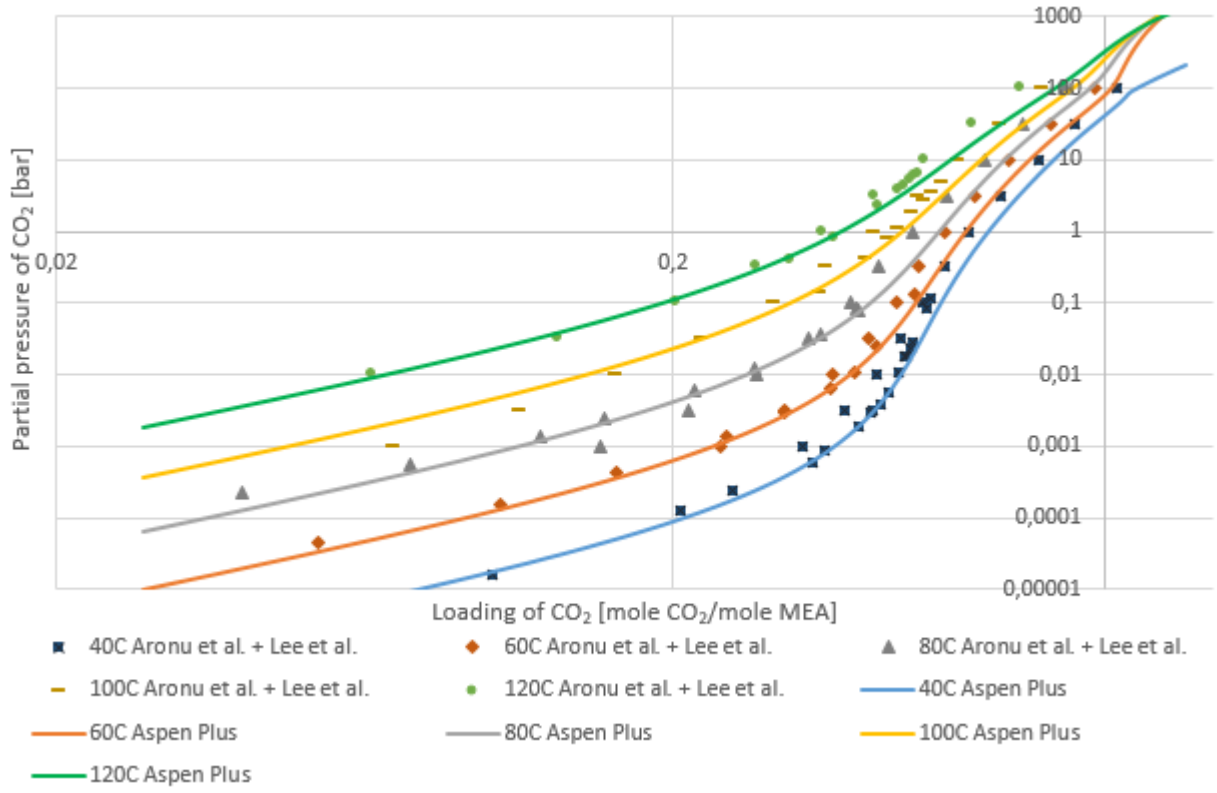

Figure 3.1.7: Aspen Plus data and experimental data from literature [30] [31] for the CO_2-MEA-H_2O system

It can be seen from the table that the model fits quite well with the experimental data. This applies for the whole temperature interval that will be used in the simulations (40-100°C). This again indicates that the model gives accurate results for the whole interval.

4 Simulation Results

All three simulations have the same basic structure, which can be seen in figure 4.0.1. The biogas enters the absorber at the bottom, at different pressures for each process. For the water-scrubbing and DEPG-scrubbing the pressure is elevated, and therefore the biogas goes through a compression train before it enters the absorber. The construction of a compression train can be seen in figure 4.0.2. The biogas streams upwards in the absorber, counter-currently with the solvent. When the cleaned biomethane exits the absorber it enters a new compressor train where it is pressurized to 80 bars and holds a temperature of 30 °C, this is to give a common criterion for the processes for fair comparison. All three processes reach the requirements, which are a methane purity of 97.5% (mole/mole) after Swedish standards [9] [10] and a maximum methane slip of 5% (mole/mole). The solvent containing the CO_2 exits the absorber at the bottom, and is heated before it enters the desorber where the CO_2 is stripped from the solvent. The CO_2 exits the process at the top of the desorber where it enters a compressor train where it is compressed to 80 bar and holds a temperature of 30 °C just as the methane product stream. The now stripped solvent is pumped back to the absorber and is used again and again in a loop. Descriptions and results for all simulations follow below.

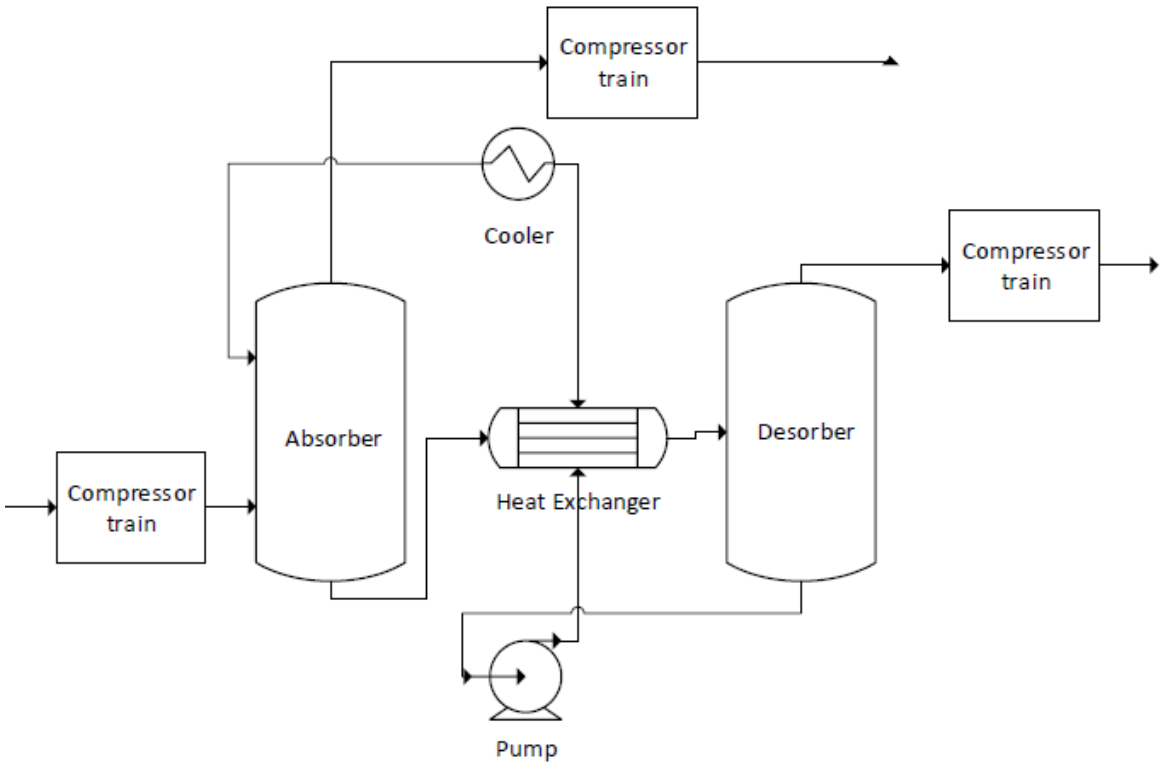

Figure 4.0.1: Generic flowsheet for the processes.

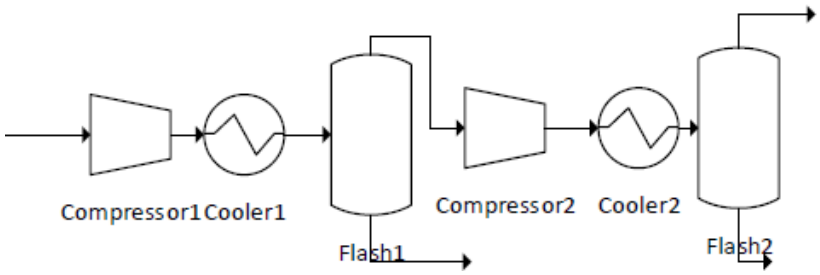

Figure 4.0.2: Compressor train.

The biogas feed-stream is identical for all three simulations and the parameters for the stream are given in table 4.0.1. The gas is saturated with water at the given conditions. All absorbers and desorbers are filled with the same structured packing, Flexipak 250Y. It is desired to find a common basis to compare the utilization of both thermal and electric energy, this can be achieved by considering that electrical energy could be generated by conversion of thermal energy using a gas turbine which has an efficiency of 40 % following [32]. To calculate the total energy consumption in terms of heat the electric energy was divided by the average typical efficiency of a gas turbine. All L/G-ratios presented are given in kg liquid/ kg gas.

Table 4.0.1: Data for the raw biogas.

Temperature [°C]	30
Pressure [bar]	1
Volume flow [m^3/h]	500
Mass flow [kg/h]	575
CH_4 fraction (%mol/mol) (dry)	60
CO_2 fraction (%mol/mol) (dry)	40

4.1 Water-scrubbing

A flowsheet of the process is given in figure 4.1.1. The biogas enters the process by being compressed to 10 bar through a compression train consisting of two compressors with intermediate cooling and separation of the condensed water. The gas then enters the absorber at the bottom and flows upwards in the column. Temperature and pressure in the column are 30 °C and 10 bars. Lean water enters the absorber at the top, flowing counter-currently downwards in the column. The cleaned gas exits the column at the top and goes through a new compressor train containing two compressors, increasing the pressure of the gas to 80 bars. The water exits at the bottom of the column and is regenerated in a regeneration cycle. The water is heated in a cross heat-exchanger before it enters at the top of the desorber, which is operated at 1 bar. The desorber is equipped with a reboiler, and here the water is heated so that the CO_2 desorb and exits the column at the top. The now clean water exits

at the bottom where it is pumped back up to 10 bars before it goes through the cross heat-exchanger, is additionally cooled and re-enters the absorber. The CO_2 gas stream enters a compression train consisting of four compressors pressurizing it to 80 bars. Table A.0.1 in appendix A shows the stream data for all streams in figure 4.1.1, wherein temperatures, pressures, moleflows, molar vapour fractions and mole-fractions of each component in the stream are given.

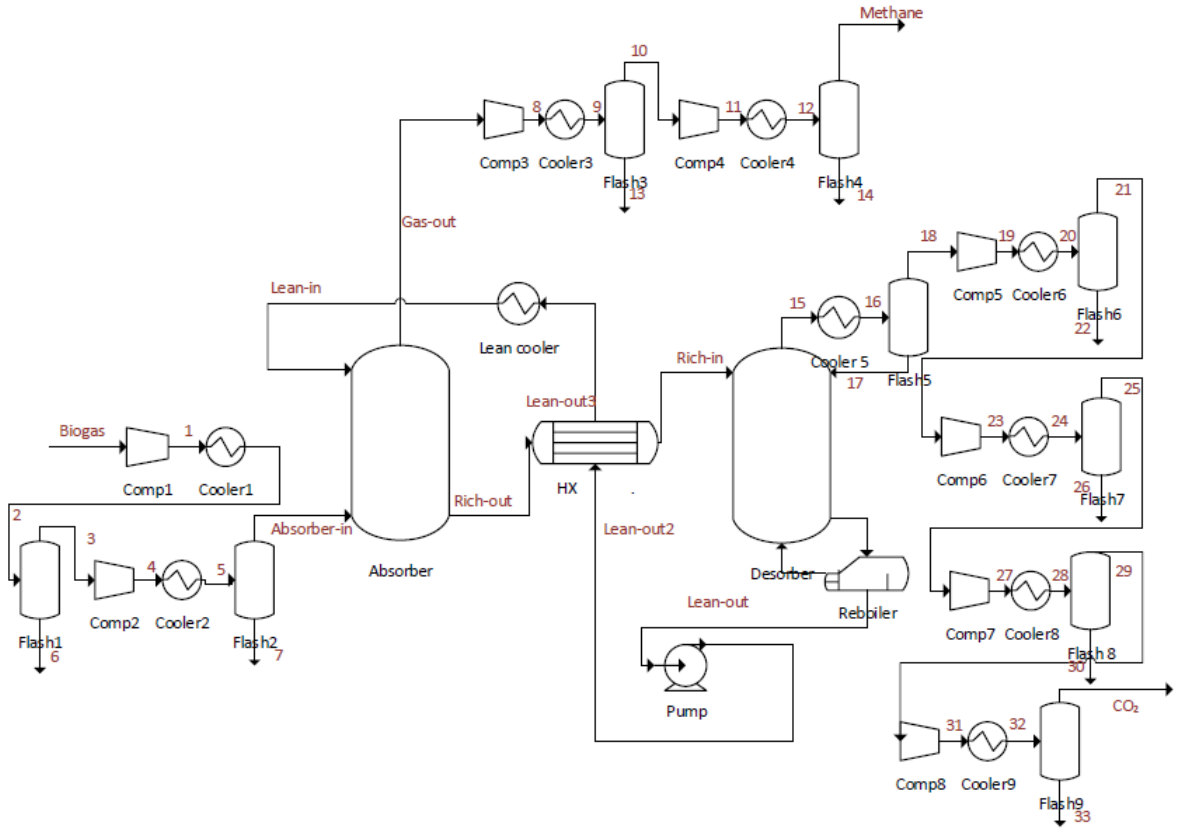

Figure 4.1.1: Flowsheet of the water-scrubbing simulation.

The simulations started with the absorber. The absorber was first tested with different heights to see at what point the height did not influence the performance of the column. This height was found to be at 10m and this was chosen for the simulations. This can be seen in figure 4.1.2. The test was done with a L/G-ratio of 120, a diameter of 0,6m and a lean loading of zero. The diameter of the column was chosen so that the flooding in the column was 80%. This diameter was used throughout all simulations.

At a height of 10m the percentage (%mole/mole) of methane in the product stream was plotted as a function of L/G-ratio to check the performance of the column. This is shown in figure 4.1.3. The methane slip (% mole/mole) of the column is also plotted as a function of L/G-ratio, which can be seen in figure 4.1.4. Parameters for the absorber are given in table 4.1.1.

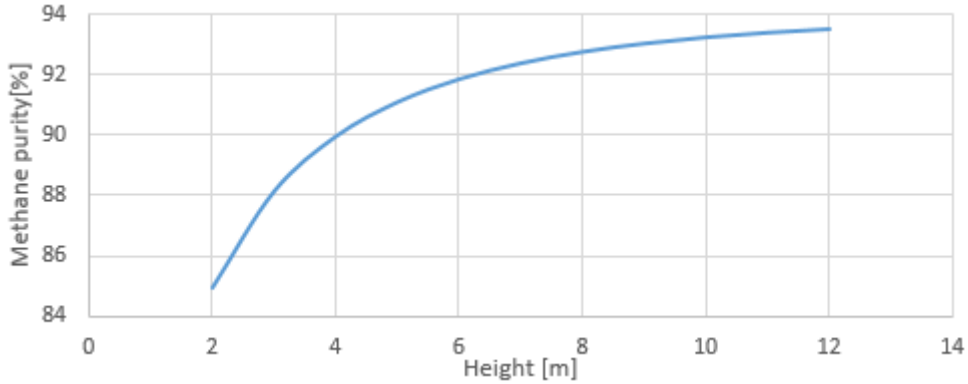

Figure 4.1.2: Percentage of methane in the product stream as a function of absorber height for the water-scrubbing simulations.

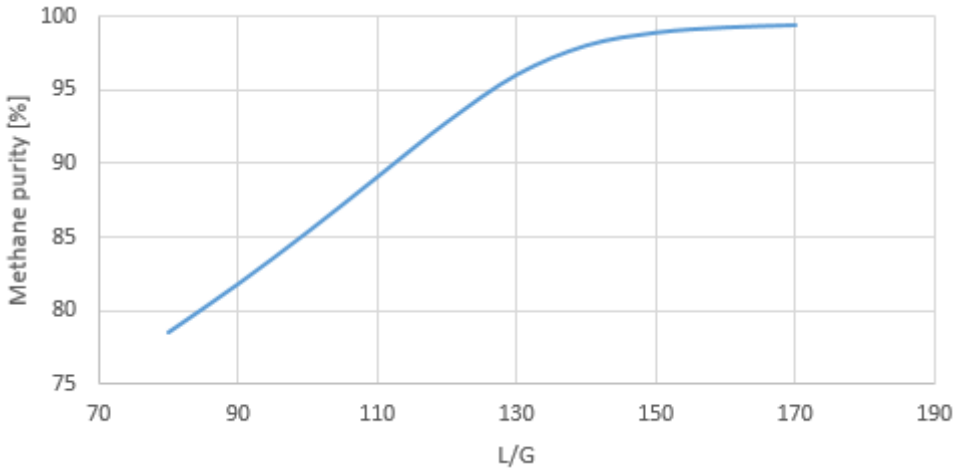

Figure 4.1.3: Methane purity of the product as a function of L/G-ratio for the water-scrubbing absorber.

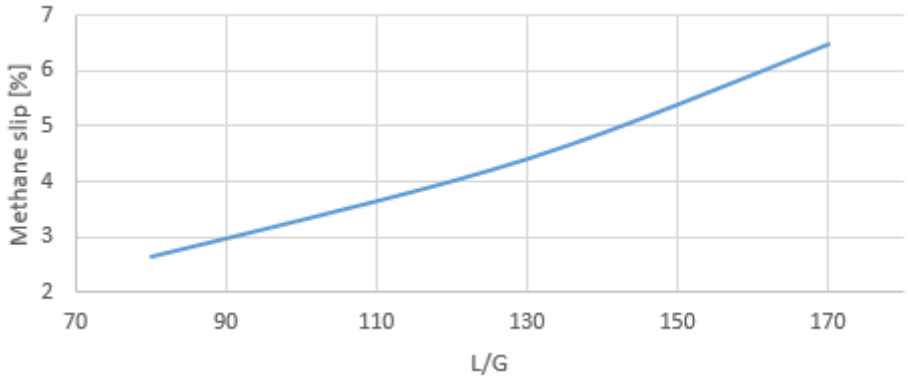

Figure 4.1.4: Methane slip as a function of L/G-ratio for the water-scrubbing simulations.

The absorber tests show that the absorber performs as expected and that to obtain the required methane purity is possible. It also shows that it is possible to achieve a low methane slip, which means that no process flash-tank between the absorber and desorber is required. This means savings in equipment cost and piping cost, not having to recycle methane back to the absorber.

A desorber with a reboiler was added to the process, together with a cross heat-exchanger between the columns. This can be seen in figure 4.1.1. The heat-exchanger operates with a ΔT_{min} of 8°C. Similar to the absorber the desorber diameter was chosen so that there was 80% flooding (0.6m) and the height was chosen to be 70% of the absorber (7m). Data for the desorber is given in table 4.1.1. To find the optimum L/G-ratio for the whole process, the reboiler duty per kg of CO_2 removed was plotted as a function of L/G-ratio, where the methane purity in the product stream was kept constant at 97.5%. The methane slip of the process was also plotted to see when the slip went above the limit of 5%. As can be seen in figures 4.1.5 and 4.1.6 the best L/G-ratio is 143 giving a reboiler duty of 8997 kJ/kg CO_2 removed, since this is the L/G-ratio giving the lowest reboiler duty while still keeping within the methane slip target of maximum 5%. This is a typical L/G-ratio for the water-scrubbing process [9]. The rich and lean loadings for the different L/G-ratios are given in figure 4.1.7.

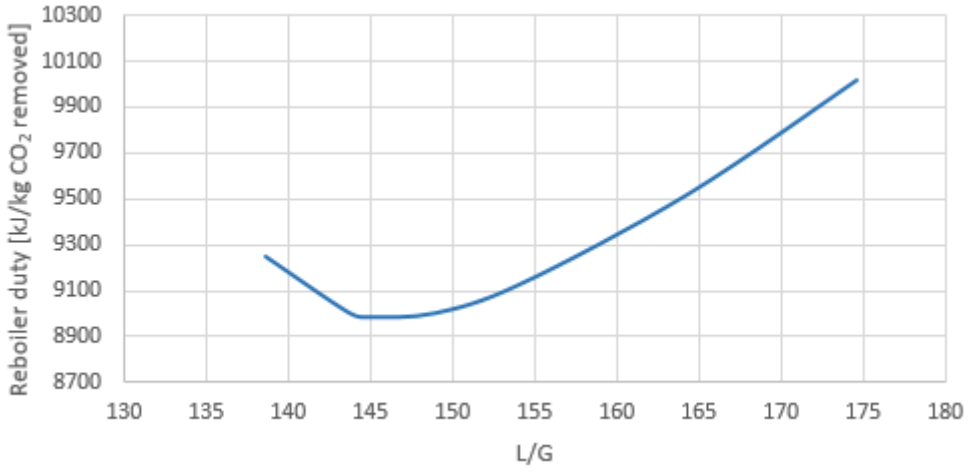

Figure 4.1.5: Reboiler duty per kg of CO_2 removed as a function of L/G-ratio for the water-scrubbing simulations.

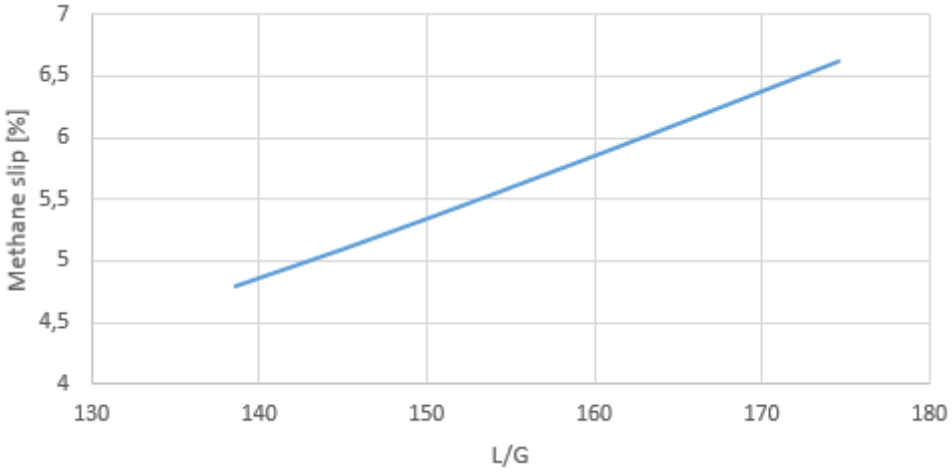

Figure 4.1.6: Methane slip as a function of L/G-ratio for the water-scrubbing simulations.

Figure 4.1.5 shows that the desorber performs as expected. For low L/G-ratios the reboiler duty required to reach the target of 97.5 % methane purity decreases with increasing reboiler

duty. This is due to the fact that with increasing amounts of water the capacity for CO_2 absorption increases. This means that the minimum required lean loading of the process increases, as more CO_2 can loop around in the system. CO_2 is easier to strip from the liquid when the loading is high, and when the loading is really low the stripping requires a lot of energy. At one point the water stream is so large that the reboiler duty starts to increase with increasing L/G-ratio, this is because the rich loading is no longer staying at its maximum capacity. When the rich loading goes down, this means that to remove all the CO_2 required to reach the target, the lean loading can no longer increase in the system. This, together with the fact that more heat is required to heat up the water to the necessary temperature, makes the required reboiler duty increase again. This results in the figure mentioned above, with a minimum reboiler duty at a specific L/G-ratio.

The methane slip increases with increasing L/G-ratio, this can be seen in figure 4.1.6. This is because with a higher L/G-ratio the absorption of both CO_2 and CH_4 increases. The methane loss is quite high, at the limit of 5%. This results in lost income, and also that the CO_2 product stream is not pure, but diluted with methane.

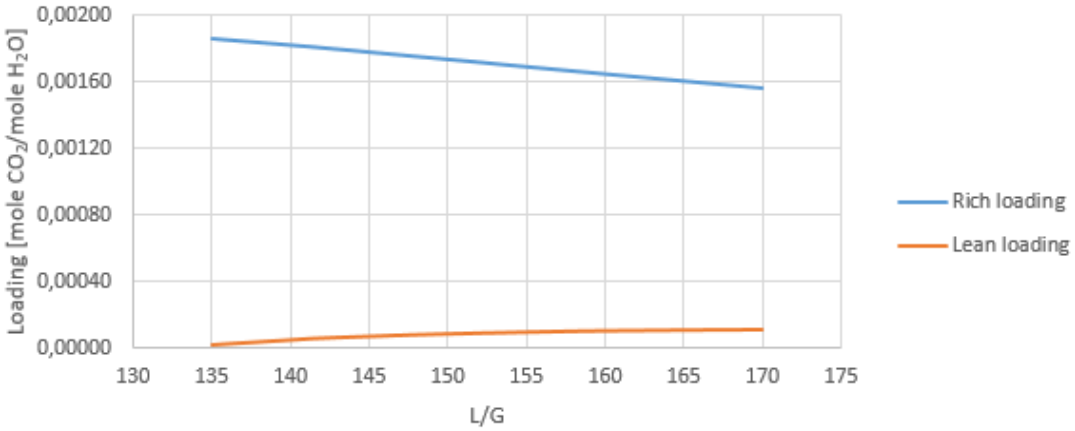

Figure 4.1.7: Rich and lean loading in the water-scrubbing simulations.

Figure 4.1.7 shows that the lean loading increases with increasing L/G-ratio. This is as described earlier due to the increasing water-stream compared to the constant flow of CO_2. The rich loading decreases at higher L/G-ratios, making the removal harder, it can be seen that when the rich loading decreases the lean loading starts to stabilize and no longer increase at the same rate.

Table 4.1.1: Parameters for the columns in the water-scrubbing simulations.

Absorber		Desorber	
Parameter	Value	Parameter	Value
Packing	Flexipak 250Y	Packing	Flexipak 250Y
Diameter [m]	0.6	Diameter [m]	0.6
Height [m]	10	Height [m]	7
Gas velocity [m/s]	0.05		
Pressure [bar]	10	Pressure [bar]	1
Gas feed [kg/h]	560		
Liquid feed [kg/h]	80080	Liquid feed [kg/h]	80439

The energy requirement for different parts of the process is given in table 4.1.2. The reboiler requires 870 kW of heat, while the coolers in the system require 1007 kW of cooling water. The cooling water is required, but due to the fact that there is large cool water-streams in the system, some of this requirement can probably be covered by a proper heat integration scheme. The heat exhanger has a capacity of 5034 kW and the pump and compressors in the system require 151 kW of electricity.

Table 4.1.2: Heat and work needed in the water-scrubbing system.

Unit	Heat [kW]	Unit	Work [kW]
HX	5034.4	Comp 1	26.7
Reboiler	870.0	Compressor 2	26.8
Cooler 1	-34.6	Compressor 3	15.3
Cooler 2	-30.0	Compressor 4	11.3
Cooler 3	-16.9	Pump	31.4
Cooler 4	-14.0	Compressor 5	10.7
Lean cooler	-733.6	Compressor 6	10.3
Cooler 5	-122.4	Compressor 7	9.9
Cooler 6	-14.0	Compressor 8	8.8
Cooler 7	-11.8		
Cooler 8	-11.8		
Cooler 9	-17.9		

The effect on the energy requirement and total cost by increasing the pressure in the absorber from 10 to 20 bars was investigated and the results are given in table 4.1.3. The number of equipment increases due to the need for extra compressors in the compressor-train before the absorber to compress the biogas to 20 bars. The L/G-ratio, reboiler duty and cooling duty needed in the process decreased, but the compressor duty and pumping duty increased. The higher pressure would also increase the cost of equipment, as it would have to hold 20 bars instead of 10bars.

Table 4.1.3: Comparison of water-scrubbing at 10 bar and 20 bar.

	10bar	20bar
Number of equipment	32	35
Best L/G	143	80
Reboiler heat duty [kW]	870.0	430.0
Compressor duty [kW]	119.8	124.4
Pump duty [kW]	31.4	39.8
Cooling duty [kW]	1007	588.9
Overall electric [kW]	151.2	164.2
Overall heat [kW]	870.0	430.0
Overall power (heat) [kW]	1248.0	840.5
Overall power (heat) [MJ/kg CO_2 removed]	13.0	8.8

4.2 Organic Solvent Scrubbing using DEPG

A flowsheet of the DEPG-scrubbing process is given in figure 4.2.1. The biogas is compressed to 8 bars in a compressor train before entering the absorber. The biogas flows upwards in the column, counter-currently with the DEPG that flows downwards. The cleaned biomethane exits the column at the top of the absorber and is compressed to 80 bars in another compressor train consisting of two compressors. The rich DEPG liquid flows into a cross heat exchanger and is heated before it enters a process flash tank at 6 bars. Here some of the methane that is absorbed is flashed off. This gas is compressed and cooled before it is recycled back to the absorber. The liquid out of the bottom of the flash-tank is further heated before it enters the desorber at the top. Here nitrogen flows counter-currently with the rich DEPG and CO_2 desorbes from the liquid. The nitrogen and CO_2 exits the column at the top of the desorber, where it is compressed to 80 bars. The now lean DEPG is recycled back to the absorber. Table A.0.2 in appendix A shows the stream data for all streams in figure 4.2.1, temperatures, pressures, moleflows, molar vapour fractions and mole-fractions of each component in the streams are given.

The simulations were started by simulating the absorber. Different heights were tested to find the height where the height did no influence the performance of the column anymore. This can be seen in figure 4.2.2, and a height of 8 meters was chosen. This test was done with a L/G-ratio of 50 and a diameter of the column of 0.4m. The lean loading was set to zero. The diameter was set so that the flooding in the column was equal to 80%, this was later adjusted to 0.5m due to the need of higher L/G-ratios than expected.

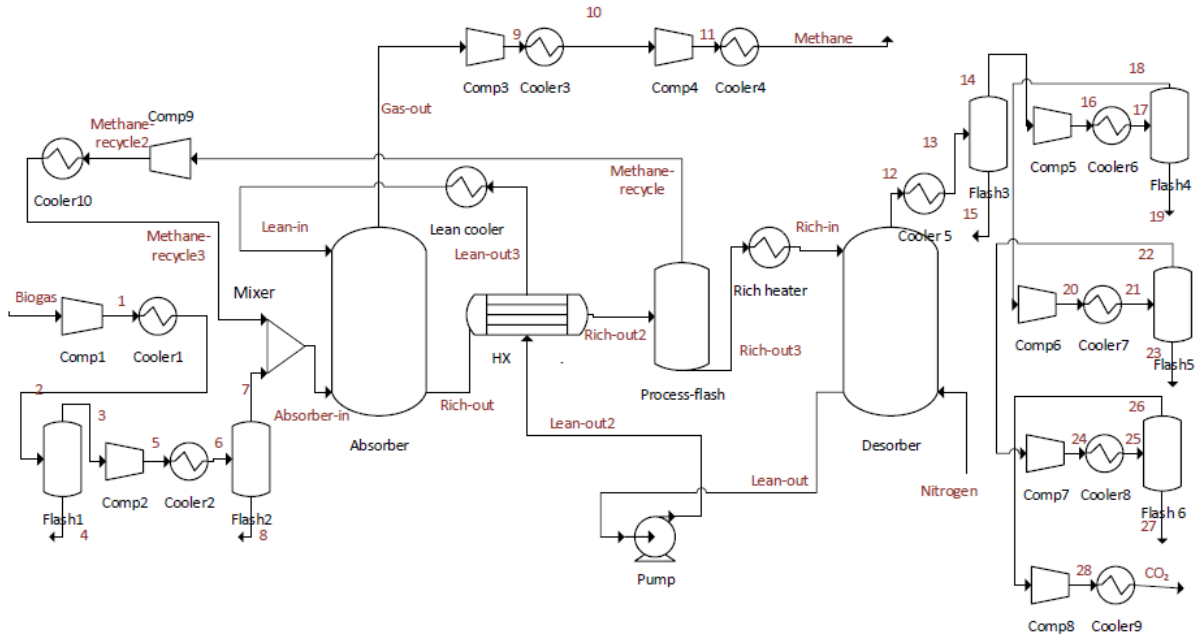

Figure 4.2.1: Flowsheet of the DEPG-scrubbing simulations.

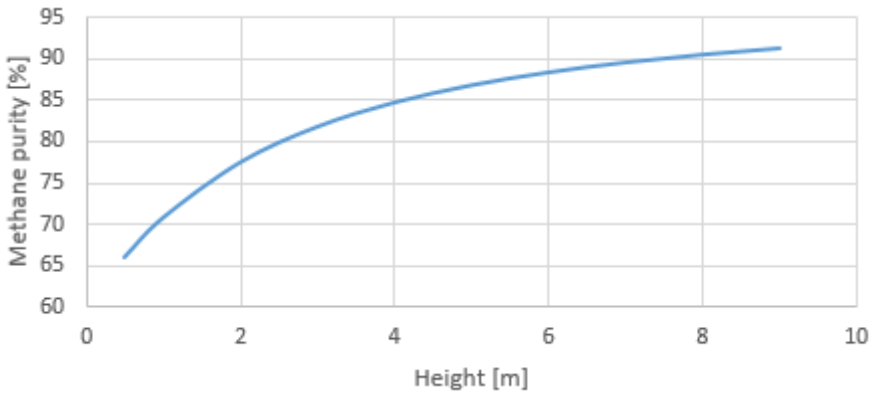

Figure 4.2.2: Percentage of methane in the product stream as a function of absorber height for the DEPG-scrubbing simulations.

When the height was determined the absorber was tested to see that it worked correctly, this was done with a temperature in the absorber of 30 and 20 °C to see if a lower temperature improved the absorption. The methane purity (% mole/mole) was plotted as a function of L/G-ratio, this can be seen in figure 4.2.3. The 20 °C case was chosen for further simulations. The methane slip (% mole/mole) was also plotted and can be seen in figure 4.2.4.

The absorber tests show that the absorber works as expected, but with a really high methane slip. When the absorber was tested for both 30 and 20 °C, it could be seen that the lower temperature resulted in higher absorption absorption, as was expected. The fact that the methane slip increases with increasing L/G-ratio is because of the same reason as in the water-scrubbing case, the more solvent there is, the better the absorption of both CO_2 and methane is going to be, resulting in more loss of methane.

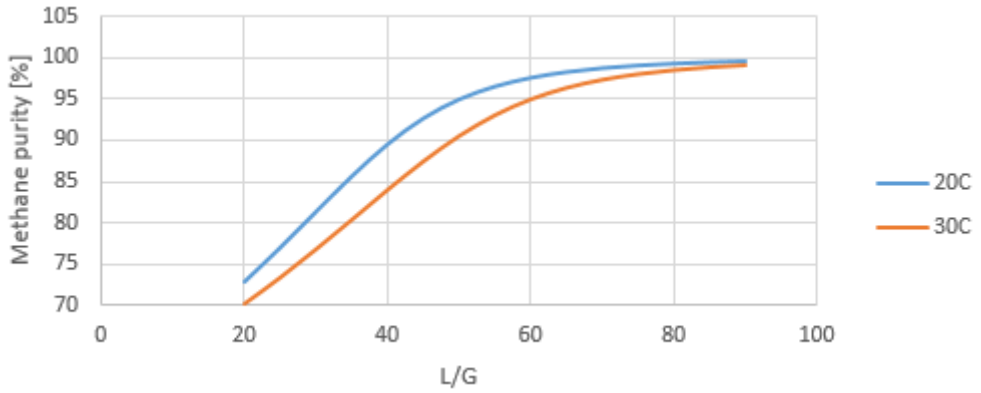

Figure 4.2.3: Methane purity as a function of L/G-ratio for 20 and 30 °C for the DEPG-scrubbing simulations.

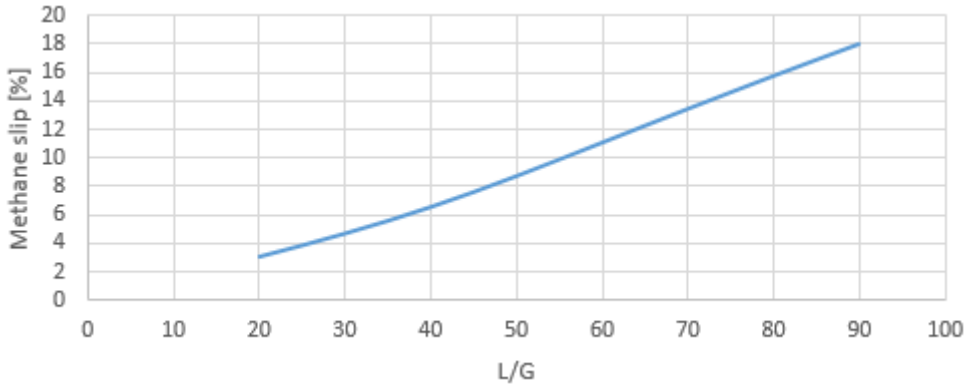

Figure 4.2.4: Methane slip plotted as a function of L/G-ratio for the DEPG-scrubbing simulations.

As the methane slip is to high, it was decided that a flash-tank would be placed after the absorber to flash off some of the methane and recycle it back to the absorber. A test at both decreasing the pressure and increasing temperature was done, and the results can be seen in figure 4.2.5.

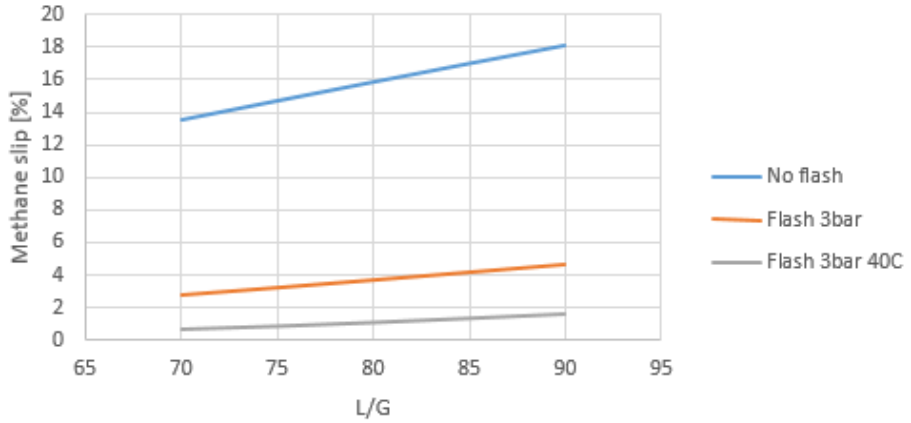

Figure 4.2.5: Methane slip as a function of L/G-ratio for the absorber-flash system with different pressures and temperatures for the DEPG-scrubbing simulations.

It can be seen from the flash-tank test that when the pressure in the flash decrease, the methane slip decreases, and it decreases additionally when the temperature is elevated. This is because when the pressure decreases or the temperature increases the solubility of methane in DEPG goes down, which leads to the desorption of methane from the DEPG. This methane can then be recirculated back to the absorber. Figure 4.2.5 shows that the flash works as expected.

The desorber was added and the cross heat-exchanger was placed between the absorber and the flash-tank with a ΔT_{min} of 8 °C. Regeneration by heat was attempted for these simulations, as in water-scrubbing by adding a reboiler in the desorber, but the temperature of the DEPG out of the desorber becomes too high. Namely higher than 175 °C which is the maximum operating temperature for DEPG [33]. It was then decided to use nitrogen stripping gas for the regeneration. The liquid is heated to 80 °C before it enters the desorber. The temperature in the flash was determined by the cross heat exchanger and different pressures in the flash-tank were tested, and the L/G-ratio giving the lowest nitrogen consumption was found for each pressure. This can be seen in figure 4.2.6.

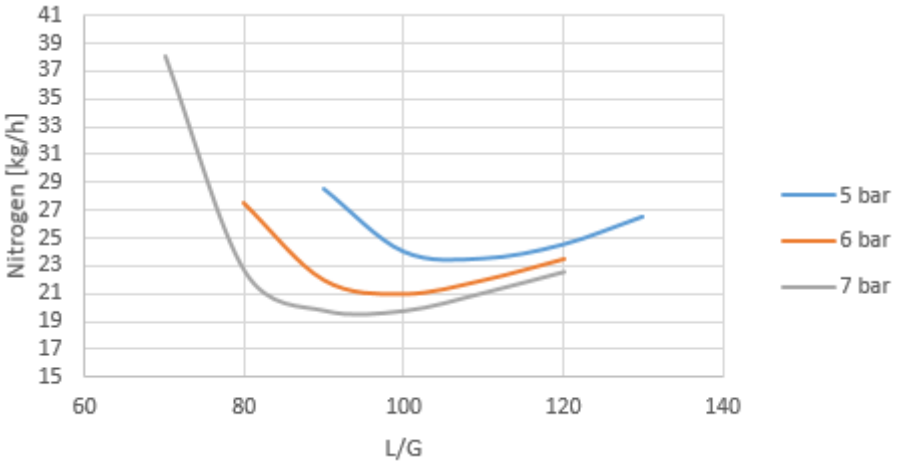

Figure 4.2.6: Nitrogen consumption as a function of L/G-ratio for different pressures in the flash-tank for the DEPG-scrubbing simulations.

As for the reboiler duty in water-scrubbing the nitrogen consumption goes down with increasing L/G-ratios at low L/G-ratios due to the fact that the CO_2 is easiest removed when the lean loading is high, and the lean loading increases with increasing L/G-ratio. This can be seen in figure 4.2.9. At one point the liquid stream is getting so large that the rich loading is getting lower, and thereby the lean loading cannot increase for higher L/G-ratios anymore. This again leads to that the nitrogen consumption starts to increase again with increasing L/G-ratio at high L/G-ratios. It can also be observed that the minimum amount of nitrogen needed decreases with increasing pressure in the flash tank. It is assumed this is because, by reducing the pressure, the possibility of recovering CO_2 merely by pressure swing is reduced.

The methane slip for each flash-tank pressure is plotted as a function of L/G-ratio in fig-

ure 4.2.7. The limit for the methane slip is set to 2.5% in this case, this is due to the underestimation of methane solubility that was found in the VLE-validation. It is assumed that using 2.5% will be equivalent with a 5% limit in reality. It can be seen in figure 4.2.6 that higher pressure gives a lower optimum nitrogen consumption, and the optimum is at a lower L/G-ratio. This is because the lower the flash pressure, the more of the absorbed methane will flash off and recycle back to the absorber. When the pressure in the flash increases the amount of methane leaving with the liquid also increases. But to keep within the methane slip requirement a pressure of 6 bar and a L/G-ratio of 100 gives the best results with a nitrogen consumption of 21 kg/h and a methane slip of 5%.

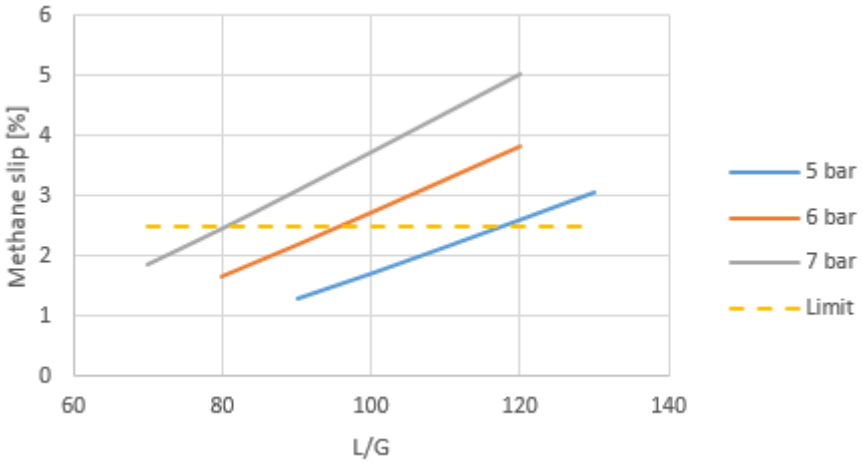

Figure 4.2.7: Methane slip as a function of L/G-ratio for different pressures in the flash-tank for the DEPG-scrubbing simulations.

The nitrogen consumption graph for 6 bars is given in figure 4.2.8 and the lean and rich loading for the process are given in figure 4.2.9. The rich loading is decreasing, making it harder to desorb the CO_2 as already mentioned in the water-scrubbing case. Here it can also be seen that the lean loading is almost constant at higher L/G-ratios, which is a consequence of the fact that the rich loading is decreasing, making the nitrogen consumption higher.

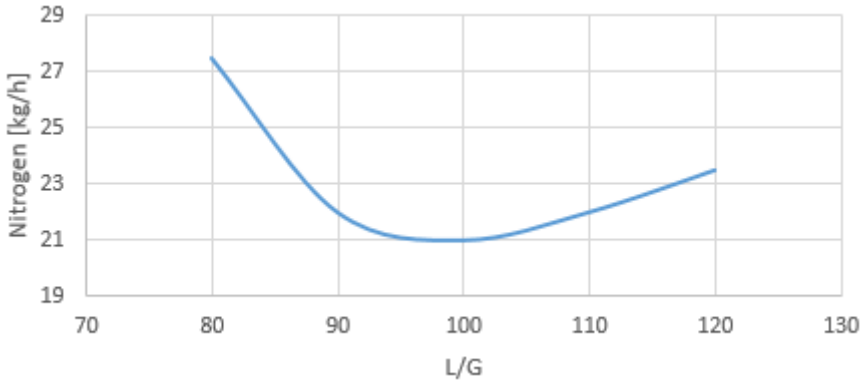

Figure 4.2.8: Nitrogen consumption as a function of L/G-ratio for the DEPG-scrubbing simulations with a fixed flash-tank pressure of 6 bars.

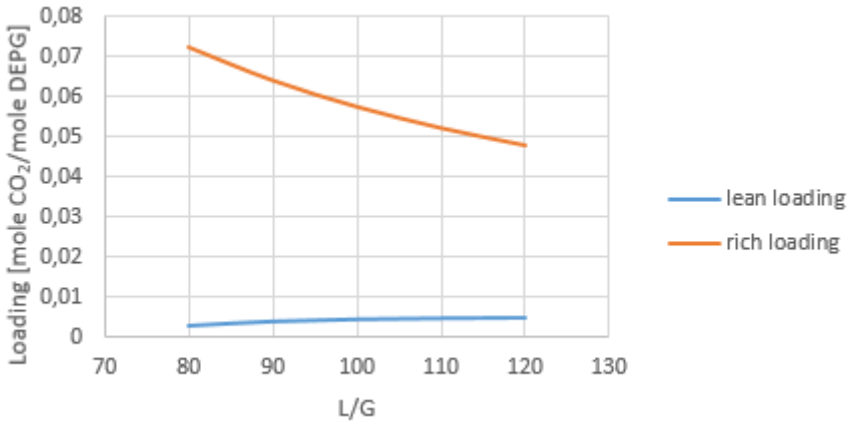

Figure 4.2.9: Lean and rich loading as a function of L/G-ratio for the DEPG-scrubbing simulations with a fixed flash-tank pressure of 6 bars.

Parameters for the absorber and desorber are given in table 4.2.1 and all required heat and work in the system is presented in table 4.2.2. Overall energy consumption for the process is given in table 4.2.3. The heater requires 306 kW of heat while a total of 481 kW of cooling duty is required. The heat exhanger has a capacity of 1759 kW while 140 kW of electricity is required for the pump and compressors of the system. This energy consumption is calculated assuming that cooling the solvent and gas down to 20 °C can be accomplished using cooling water. This is reasonable in Norway, but will no be possible in other climates.

Table 4.2.1: Parameters for the columns in the physical absorption with DEPG-scrubbing simulations.

Absorber		Desorber	
Parameter	Value	Parameter	Value
Packing	Flexipak 250Y	Packing	Flexipak 250Y
Diameter [m]	0.5	Diameter [m]	0.5
Height [m]	8	Height [m]	5.6
Gas velocity [m/s]	0.106		
Pressure [bar]	8	Pressure [bar]	1
Gas feed [kg/h]	560	Gas feed [kg/h]	21
Liquid feed [kg/h]	56000	Liquid feed [kg/h]	56355

Table 4.2.2: Heat and work needed in the DEPG-scrubbing system.

Unit	Heat [kW]	Unit	Work [kW]
HX	1759.2	Compressor 1	25.8
Heater	305.9	Compressor 2	22.9
Cooler 1	-33.1	Compressor 3	15.9
Cooler 2	-28,6	Compressor 4	14,1
Cooler 3	-15.8	Compressor 5	11.4
Cooler 4	-17.2	Compressor 6	10.8
Lean cooler	-324.5	Compressor 7	10.5
Cooler 5	-4.9	Compressor 8	9.5
Cooler 6	-11.6	Compressor 9	1.6
Cooler 7	-11.6	Pump	17.1
Cooler 8	-12.6		
Cooler 9	-16.6		
Cooler 10	-4.2		

Table 4.2.3: Summary of needed energy in the DEPG-scrubbing system.

Number of equipment	33
Best L/G	100
Reboiler heat duty [kW]	0
Compressor duty [kW]	122.5
Pump duty [kW]	17.1
Cooling duty [kW]	480.7
Heating duty [kW]	305.9
Overall electric [kW]	139.6
Overall heat [kW]	305.9
Overall power (heat) [kW]	654.9
Overall power (heat) [MJ/kg CO_2 removed]	6.8

4.3 Amine Scrubbing using MEA

A flowsheet of the process is given in figure 4.3.1. The biogas enters at the bottom of the absorber and flows upwards, while the lean solution enters at the top and flows counter-currently downwards in the column. The temperature and pressure in the column are 30 °C and 1 bar. The cleaned gas exits at the top of the column, it is cooled and separated so that the vaporized solvent is returned to the absorber. The gas is then compressed through 4 compressors, with intermediate cooling, to 80 bars. The rich solution exiting the absorber is heated by the lean solution from the desorber in a cross heat-exchanger. The rich solution then enters the desorber and the CO_2 desorb from the solution. The gas out of the desorber is cooled and the condensed liquid is circled back to the desorber. The gas is compressed in 4 compressors, with intermediate cooling, to 80 bars. The lean solvent leaving the desorber

at the bottom is cooled before it re-enters the absorber. Table A.0.3 in appendix A shows the stream data for all streams in figure 4.3.1, temperatures, pressures, moleflows, molar vapour fractions and mole-fractions of each component in the stream are given.

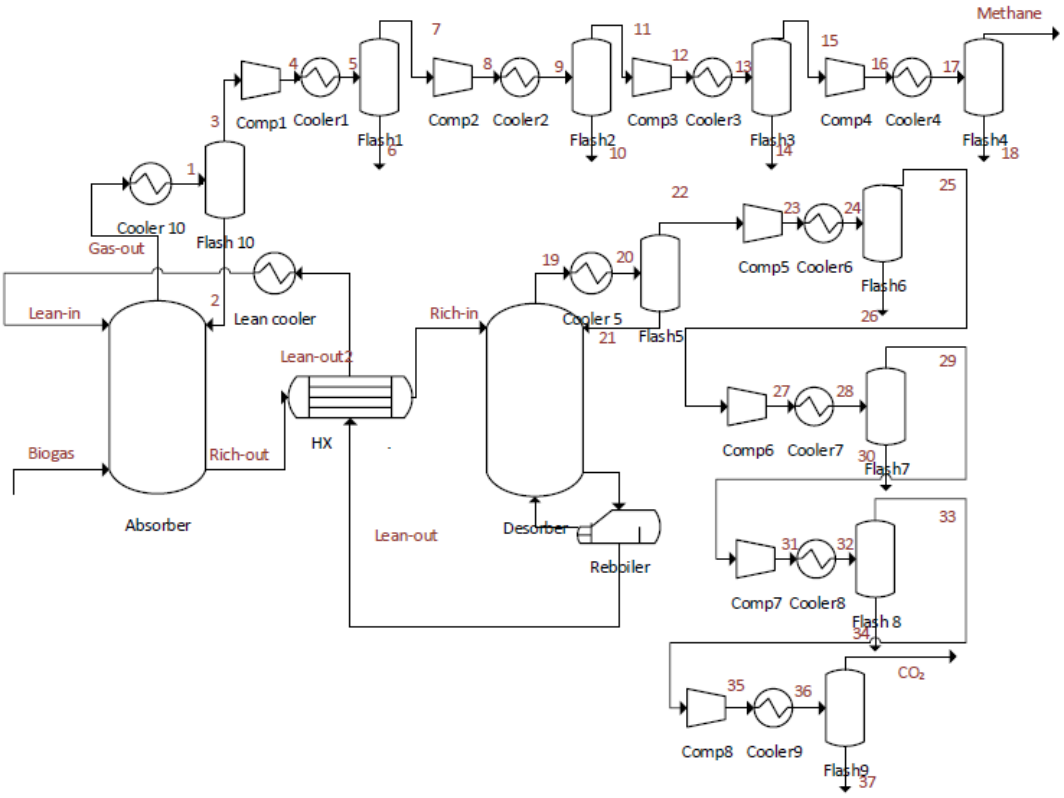

Figure 4.3.1: Flowsheet of the MEA-scrubbing case.

To determine the height of the absorber column the column was simulated with different heights at a constant L/G-ratio of 8 to see when the height did not influence the absorption performance, this can be seen in figure 4.3.2. Fourteen (14) meters was chosen. The diameter of the column was 0.4m, to gave 80% flood in the column. This diameter was used throughout all the simulations. The lean loading into the column was set to 0.2 mole CO_2/ mole MEA .

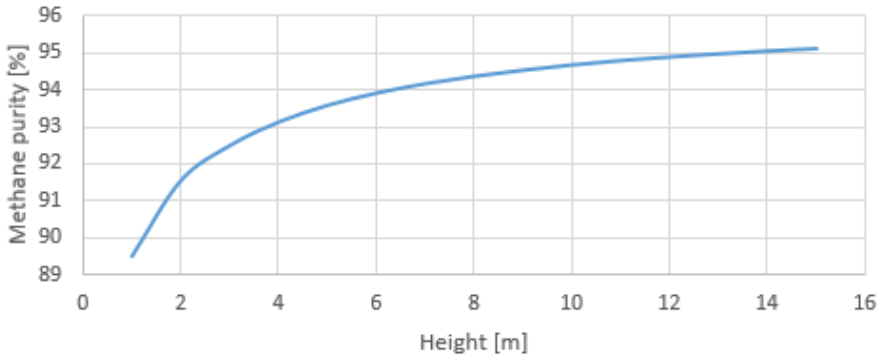

Figure 4.3.2: Methane purity of the product gas as a function of absorber height for the absorber in the MEA-scrubbing simulations.

At the set height the absorber column was tested for different L/G-ratios to see how the column performed. The methane purity (% mole/mole) and the methane slip (% mole/mole) of the column can be seen in figures 4.3.3 and 4.3.4. The temperature profile for the column at different L/G-ratios was also studied, and can be seen in figure 4.3.5.

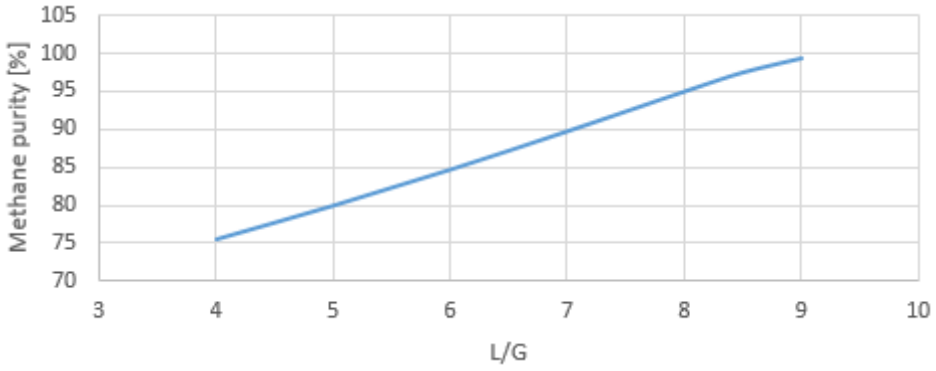

Figure 4.3.3: Methane purity in the product gas as a function of L/G-ratio for the absorber in the MEA-scrubbing simulations.

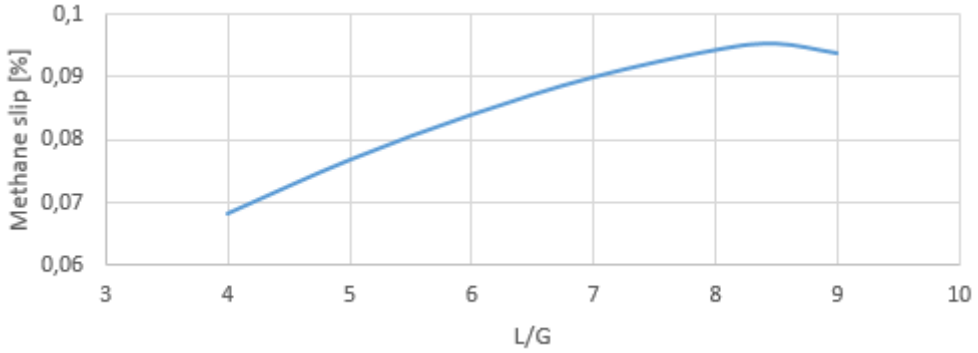

Figure 4.3.4: Methane slip for the absorber alone in the MEA-scrubbing simulations.

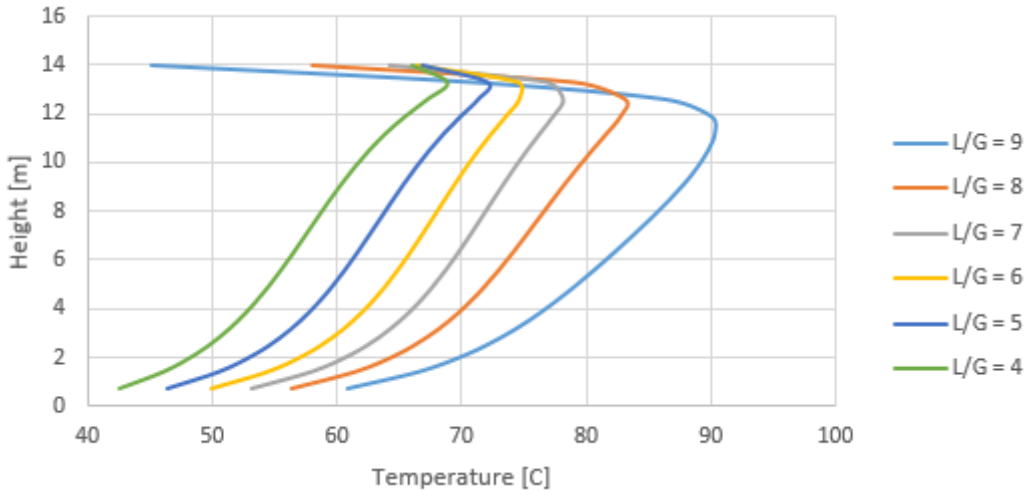

Figure 4.3.5: Temperature profiles for different L/G-ratios for the absorber in the MEA-scrubbing simulations.

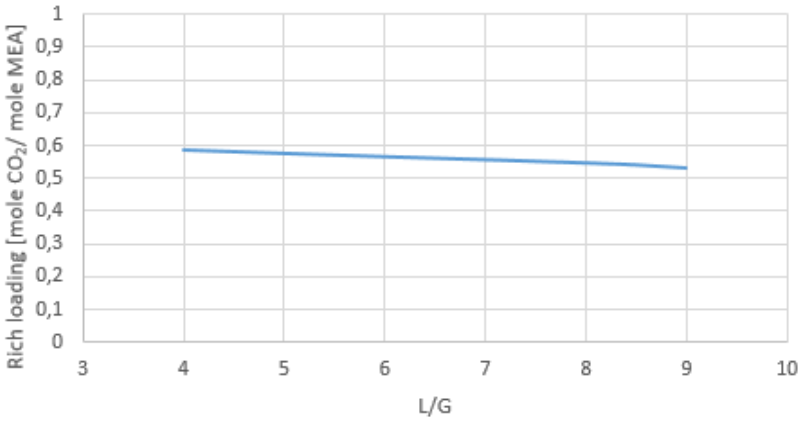

Figure 4.3.6: Rich loading in the absorber for the MEA-scrubbing simulations.

The absorber tests show that the absorber works as was expected. The test shows that the desired methane purity is possible to reach, and figure 4.3.4 shows that the methane slip for this case is really low. This is because in chemical absorption the majority of the absorption happens through chemical reactions. These reactions are between CO_2 and MEA. The only way that methane is absorbed is through physical absorption in the water. The L/G-ratio is a lot lower for chemical absorption compared to in water- and DEPG-scrubbing, and thereby there is a lot less methane that can possibly be absorbed. The temperature in the column increases with increasing L/G-ratio. This is expected as more of the CO_2 reacts at once at the top of the column. It was investigated if inter-cooling would help the absorption as the temperature in the column is so high, but as can be seen in figure 4.3.6 the rich loading is at the maximum value for MEA (this maximum value is a bit above 0.5 due to the stoichiometry of the reactions shown before in table 3.0.1), so the inter-cooling would not help the absorption. This means money is saved in not needing additional piping or extra equipment.

As for the other simulations a desorber with a reboiler was added to the simulations, with a cross heat-exchanger connecting the two columns. A flowsheet of the process can be seen in figure 4.3.1. The heat-exchanger operates with a ΔT_{min} of 8 °C as before and the diameter of the desorber is set to 0.4 m to achieve the 80% of flooding. The height of the desorber was chosen to be 70% of that of the absorber. Data for the desorber can be found in table 4.3.1. The required reboiler duty as a function of L/G-ratio to achieve the specified target of 97.5% pure methane in the product stream is given in figure 4.3.7, the corresponding loadings are given in figure 4.3.8. The simulations did not converge for higher L/G-ratios than 9.5, so this was chosen as the best ratio. The required reboiler duty is then 3759 kJ/kg CO_2 removed.

Figure 4.3.7 shows that the system performs as expected. At low L/G-ratios the reboiler duty required to reach the methane purity target decreases with increasing L/G-ratio. As the simulations do not converge for higher L/G-ratios than 9.5 the assumed trend that the reboiler

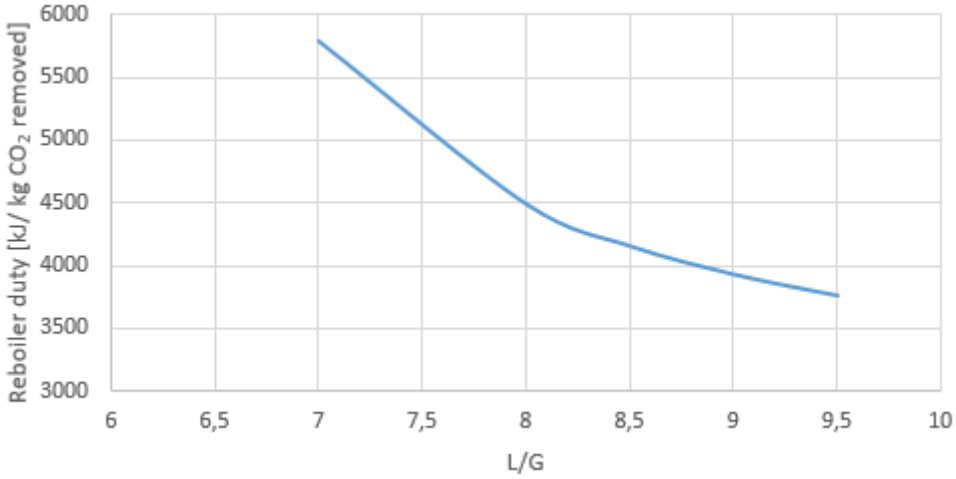

Figure 4.3.7: Reboiler duty per kg of CO_2 removed as a function of L/G-ratio for the MEA-scrubbing simulations.

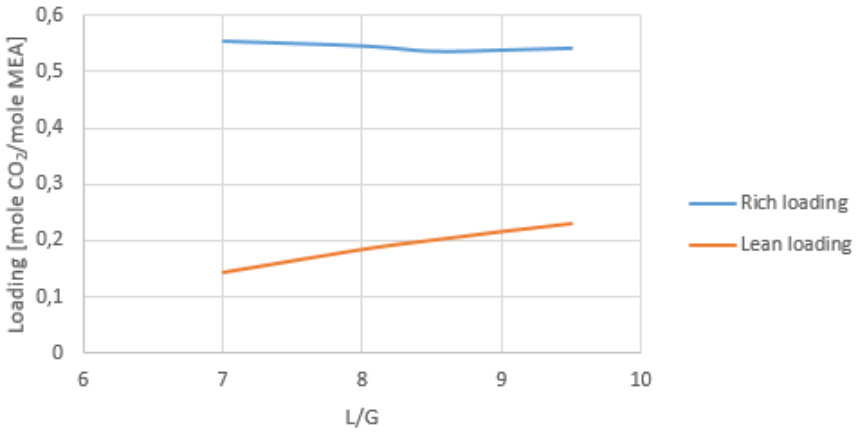

Figure 4.3.8: Lean and rich loading as a function of L/G-ratio MEA-scrubbing simulations.

duty would increase again at higher L/G-ratios can not be confirmed. However, it is assumed that, as in water-scrubbing, the reboiler duty would start to increase again as the L/G-ratio gets so high that the rich loading would not be at maximum value anymore. The rich and lean loadings can be seen in figure 4.3.8 and it can be seen that the rich loading is kept constant at a high value while the lean loading is increasing with increasing L/G-ratio. This is consistent with figure 4.3.7. The increasing lean loading makes the CO_2 easier to strip from the solvent, as fine removal requires the most energy.

The methane slip is plotted in figure 4.3.9 and it can be seen that this is well below the limit of 5% as expected. The methane does not react with the MEA, meaning that the methane is only absorbed through physical absorption in the solvent. As so little solvent is used in chemical absorption compared to physical absorption the amount of absorbed methane is really low. This means that this case has the purest CO_2 stream of all of the cases studied, its conditions are the best for CCS.

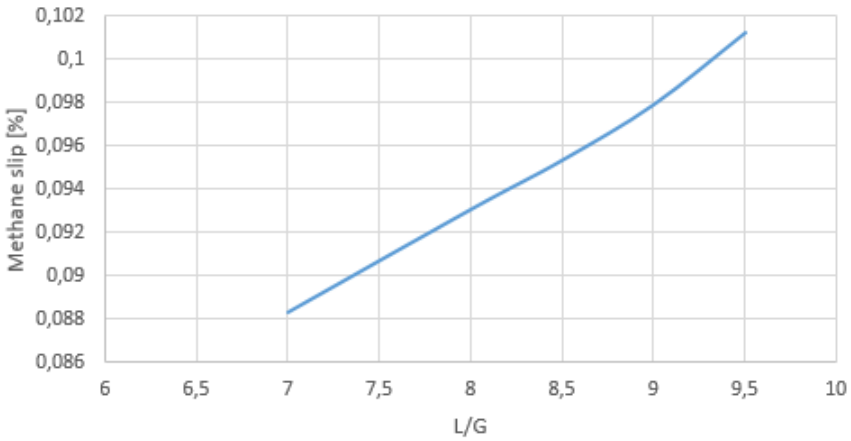

Figure 4.3.9: Methane slip as a function of L/G-ratio for the MEA-scrubbing simulations.

Parameters for the absorber and desorber are given in table 4.3.1. All required heat and work in the system are given in table 4.3.2 and overall energy consumption is given in table 4.3.3. The reboiler requires 363kW while the total cooling requirement is 484kW. The heat exchanger has a capacity of 194kW and 97kW is required in electricity for compressors and pump.

Table 4.3.1: Parameters for the columns in the MEA-scrubbing simulations.

Absorber		Desorber	
Parameter	Value	Parameter	Value
Packing	Flexipak 250Y	Packing	Flexipak 250Y
Diameter [m]	0.4	Diameter [m]	0.4
Height [m]	14	Height [m]	9.8
Gas velocity [m/s]	1.19		
Pressure [bar]	1	Pressure [bar]	1
Gas feed [kg/h]	575		
Liquid feed [kg/h]	5462.5	Liquid feed [kg/h]	5816.8

Table 4.3.2: Heat and work needed in the MEA-scrubbing system.

Unit	Heat [kW]	Unit	Work [kW]
HX	193.6	Compressor 1	15.9
Reboiler	363.0	Compressor 2	15.4
Cooler 1	-20.6	Compressor 3	15.1
Cooler 2	-17.2	Compressor 4	14.5
Cooler 3	-16.6	Compressor 5	9.9
Cooler 4	-17.7	Compressor 6	9.5
Lean cooler	-195.8	Compressor 7	9.1
Cooler 5	-137.1	Compressor 8	8.0
Cooler 6	-13.0		
Cooler 7	-11.0		
Cooler 8	-11.1		
Cooler 9	-13.5		
Cooler 10	-30.1		

Table 4.3.3: Summery of needed energy in the MEA-scrubbing case.

Number of equipment	33
Best L/G	9.5
Reboiler heat duty [kW]	363.0
Compressor duty [kW]	97.4
Pump duty [kW]	0.0
Cooling duty [kW]	483.7
Overall electric [kW]	97.4
Overall heat [kW]	363.0
Overall power (heat) [kW]	606.5
Overall power (heat) [MJ/kg CO_2 removed]	6.3

5 Economic Analysis Results

The cost of the equipment was calculated for each case. The results of the analysis and the total investment cost is presented below. Equipment cost was calculated using equation 5.0.1 [34], where A, B and n are constants and S is a unit of size for the equipment. Equation 5.0.2 [35] was used in cases where the equipment was outside of the size interval for equation 5.0.1. Here A is a unit of size for the equipment and K_1, K_2 and K_3 are constants. The constants and how the size of the equipment was calculated for every component is given in appendix B.

$$Cost = A + B \cdot S^n \tag{5.0.1}$$

$$log_{10}Cost = K_1 + K_2 log_{10}(A) + K_3 log_{10}(A)^2 \tag{5.0.2}$$

The utility prices used in this analysis are given in table 5.0.1. The electricity price is the average of the last 5 years in Norway. The steam was assumed to be low pressure steam at 5 bar. It was assumed that the plant is in Norway and that cooling water would be free, using sea water. There would be a need for filtration of this water before it is used, so a small cost would occur, which is neglected. The price of raw materials and products used are also given in table 5.0.1. Where the price of methane is the average price of 2018 for natural gas in the EU. The CO_2 price is the market price given by the Global CCS Institute and the price of the biogas entering the process is set to zero. It was assumed that the solvent would be replaced once a year.

Table 5.0.1: Price of utilities, raw materials and products for the processes.

Utility	Price
Electricity [36]	0.033 USD/kWh
Steam [34]	7.31 $USD/tonne$
Fresh water[37]	1.63 USD/m^3
MEA [38]	1628.00 $USD/tonne$
DEPG [39]	1488.00 $USD/tonne$
N_2 [40]	0.46 USD/m^3
Methane [41]	0.36 USD/Sm^3
CO_2 [42]	15.00 $USD/tonne$

It was assumed that one operator would have to be hired to work the plant, additional staff is assumed employed at the plant before the gas-cleaning process is acquired. It was assumed that the disposal of the chemicals (MEA and DEPG) would cost the same as the price to

purchase them. Annual maintenance was set to 4% of the ISBL and the property taxes and insurance was set to 2% of the fixed capital. The depreciation rate for the plants was set to 20% and declining-balance depreciation was used.

The lifetime of the plant was set to 10 years. The payback time was found and the internal rate of return and the return on investment was calculated. How this was calculated can be seen in appendix C. A sensitivity analysis of the investment analysis was performed for all three processes. The effect of change in methane price, biogas price, CO_2 price and a change in the investment cost is studied.

5.1 Water-scrubbing

The cost of all equipment is presented in table 5.1.1 and the distribution of the cost is presented in figure 5.1.1. The cost of the absorber and desorber is the combined cost of the vessel shell and the packing inside. The cost of the coolers is the combined cost of all 10 coolers in the system, the compressor cost is the combined cost of all 8 compressors in the system and the flash-tank cost is the combined cost of all 9 flash-tanks. The material of the equipment used is carbon steel. The variable cost of the water-scrubbing plant are given in table 5.1.2, the income in the water-scrubbing case are given in table 5.1.3 and the fixed cost is given in table 5.1.4

Table 5.1.1: Investment cost for the water-scrubbing case.

Equipment	Calculated cost [USD]	ISBL [USD]	Investment cost [USD]
Absorber	48 873	156 395	284 638
Desorber	39 020	124 865	227 254
Heat exhanger	189 470	606 303	1 103 472
Coolers	322 549	1 032 155	1 878 523
Pump	12 425	39 759	72 361
Reboiler	36 712	117 477	213 808
Compressors	146 502	472 007	859 052
Flash-tanks	61 469	196 700	357 993
SUM	858 019	2 745 660	4 997 101

It can be observed that all the coolers in the system accounts for the biggest equipment cost, but the most expensive single unit is the cross heat-exhanger between the absorber and the desorber in the flowsheet. The pump is the smallest equipment cost for this case together with the flash-tanks used in the compressor-trains.

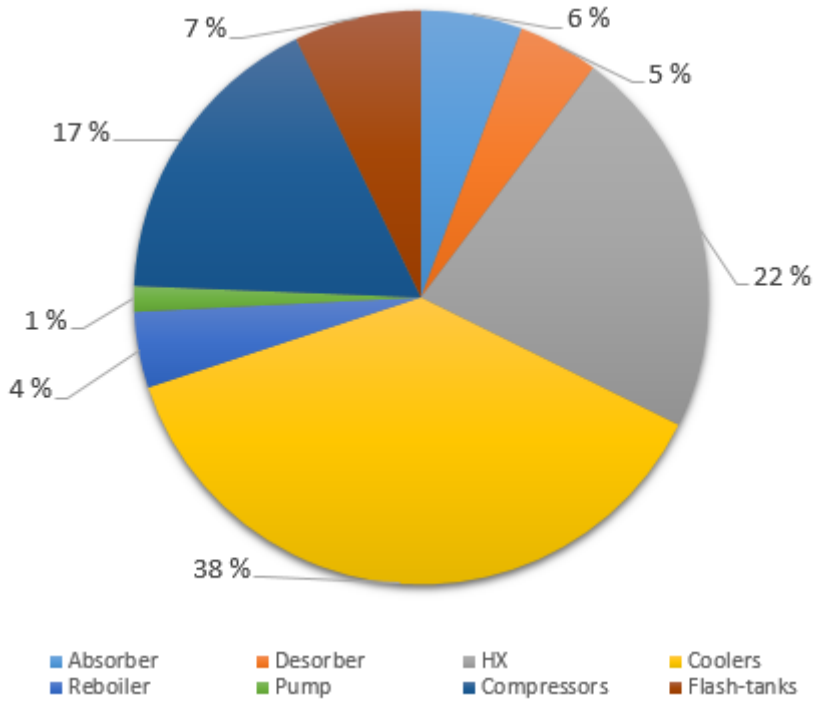

Figure 5.1.1: Distribution of the total equipment cost in water-scrubbing plant.

Table 5.1.2: Variable cost for the water-scrubbing case.

Item	Total consumption	Cost [USD/year]
Electricity	1 324 512 $kWh/year$	43 314
Steam	13 019 $tonne/year$	95 168
Water	54 $m^3/year$	87
Total		138 569

Table 5.1.3: Income for the water-scrubbing case.

Product	Production	Income [USD/year]
Methane	2 676 293 $m^3/year$	966 834
CO_2	3 051 $tonne/year$	45 764
Total		1 012 598

Table 5.1.4: Fixed costs in the water-scrubbing case.

Fixed cost	Calculated as	Cost [USD]
Property taxes and insurance	2% of fixed capital	99 942
Depreciation	20%	
Annual maintenance	4% of ISBL	109 826
Operator cost (salary)	40 000 USD/operator	40 000
Total		249 768

The result of the investment analysis can be seen in figure 5.1.2. As can be seen in the figure the payback time of the plant is 9 years. The internal rate of return (IRR) was calculated to 1.51% and the return of investement (ROI) was calculated to be 1.09%.

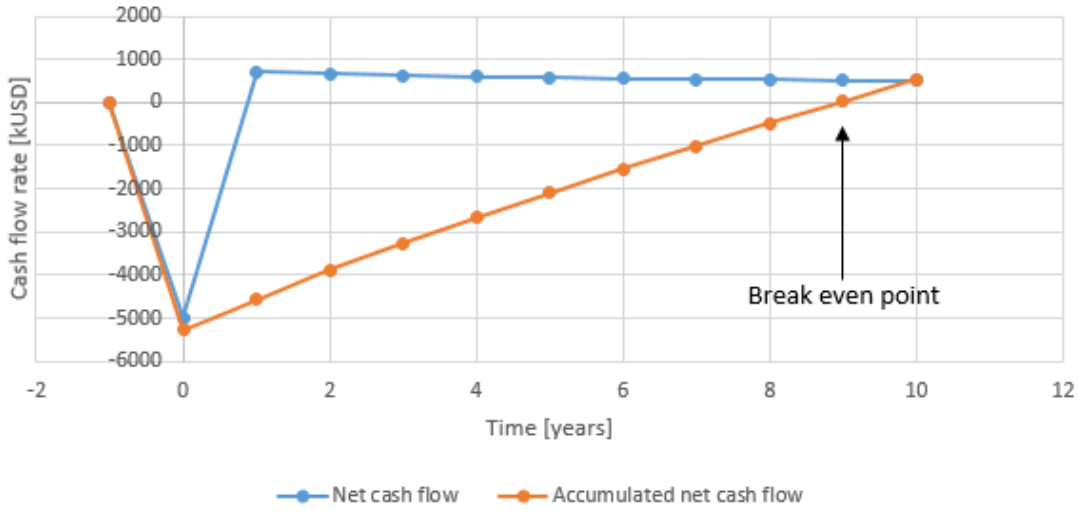

Figure 5.1.2: Net cash flow and accumulated net cash flow for the water-scrubbing plant.

A sensitivity analysis was performed and can be seen in figures 5.1.3, 5.1.4, 5.1.5 and 5.1.6. A trendline is added so that the slope of the function is clear for comparison with the other plants. It can be seen that the IRR decreases with increasing investment cost as expected. The same applies for the increase in the price of biogas. The IRR increases with increasing methane and CO_2 prices, as the income increases when these prices increase. The change in the system as the CO_2 price gets lower is especially interesting since the purity of the CO_2 stream in this case is not the best. It can be expected that the income from CO_2 will be lower than the initially given price, meaning the IRR will be lower than calculated in the investment analysis. It can be observed however, that the IRR is more sensitive to change in the methane price than in the CO_2 price.

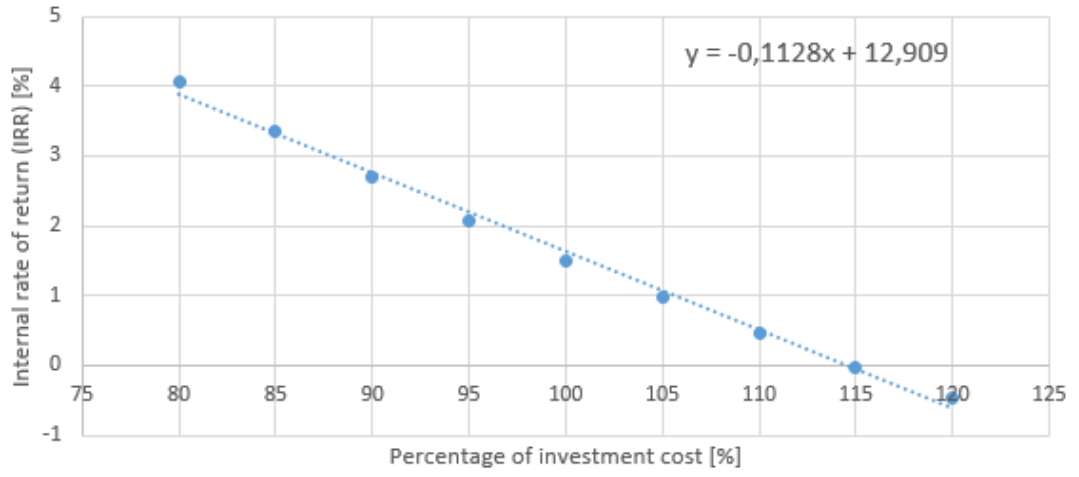

Figure 5.1.3: IRR as a function of the investment cost for the water-scrubbing plant.

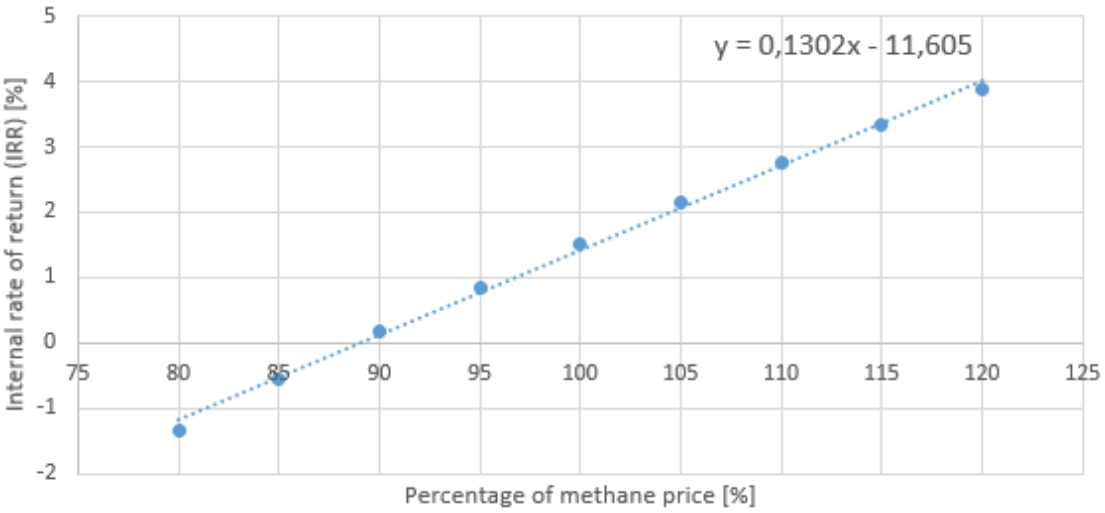

Figure 5.1.4: IRR as a function of methane price for the water-scrubbing plant.

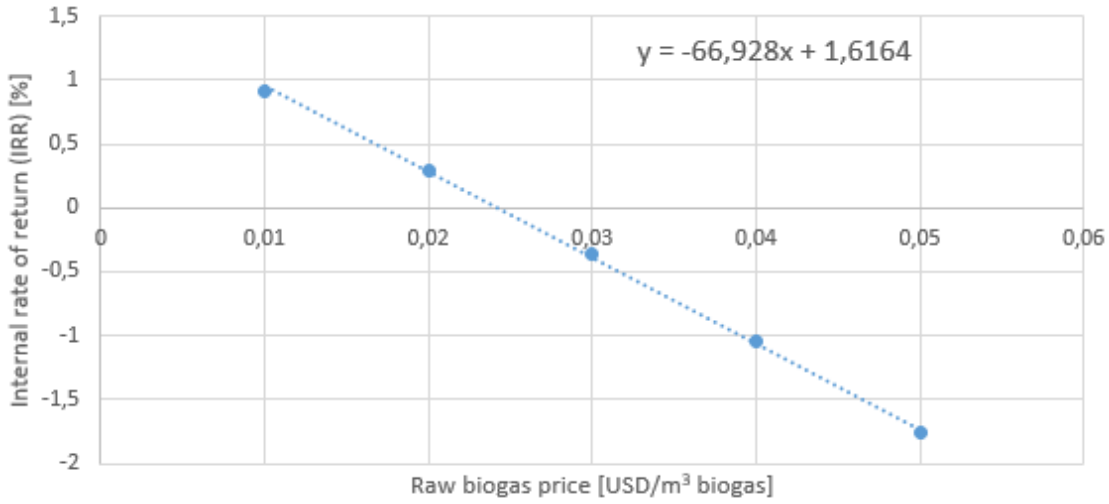

Figure 5.1.5: IRR as a function of biogas price for the water-scrubbing plant.

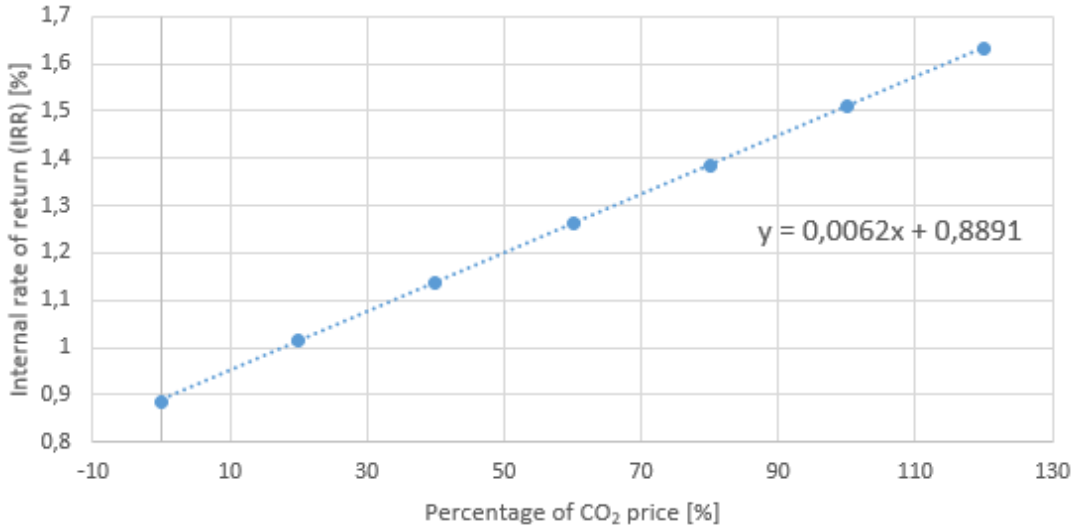

Figure 5.1.6: IRR as a function of CO_2 price for the water-scrubbing plant.

5.2 Organic Solvent Scrubbing using DEPG

The cost of all equipment is presented in table 5.2.1 and the distribution of the cost between different equipment is presented in figure 5.2.1. The cost of the absorber and desorbers includes the cost of packing, the cooler cost is the combined cost of all coolers, and the same applies to the compressors and the flash-tanks. The material used in these calculations is carbon steel. The variable costs of the process are given in table 5.2.2, the fixed cost are presented in table 5.2.4 and the income of the process is given in table 5.2.3.

Table 5.2.1: Investment cost for the DEPG-scrubbing case.

Equipment	Calculated cost [USD]	ISBL [USD]	Investment cost [USD]
Absorber	34 950	111 840	203 550
Desorber	29 045	92 945	169 159
Heat exhanger	176 979	566 331	1 030 723
Coolers	328 829	1 052 254	1 915 102
Pump	9 212	29 480	53 653
Heater	29 430	94 175	171 399
Compressors	165 981	531 138	966 672
Flash-tanks	19 319	61 822	112 517
Process flash-tank	20 686	66 194	120 473
SUM	814 431	2 606 180	4 743 247

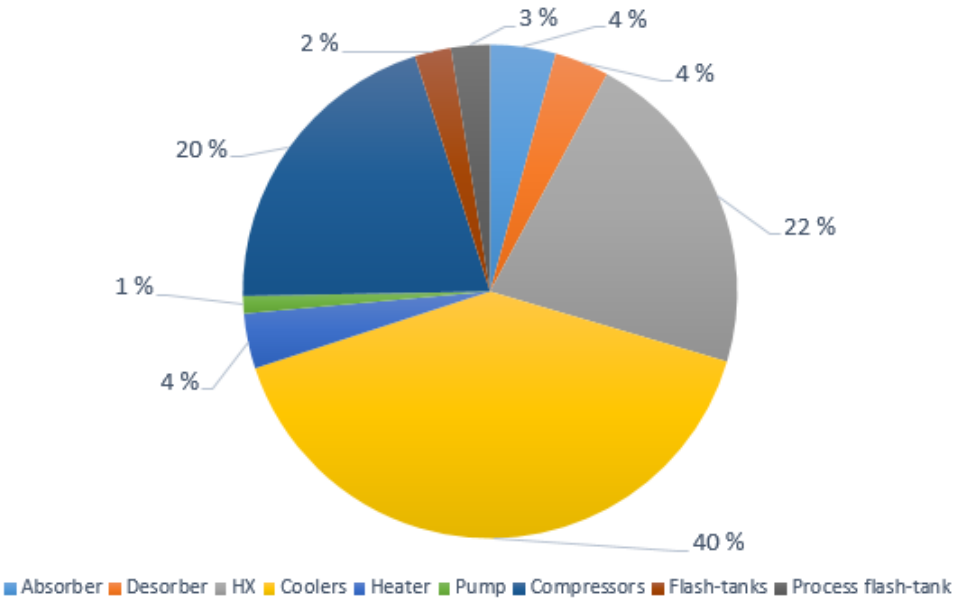

Figure 5.2.1: Distribution of the total equipment cost in DEPG-scrubbing plant.

In this case, as in the water-scrubbing case, the most expensive equipment are the coolers, and the most expensive single unit of equipment is the cross heat-exhanger, accounting for 22% of the cost. The cheapest equipment are the pump and the flash-tanks in the compressor trains.

Table 5.2.2: Variable cost for the DEPG-scrubbing case.

Item	Total consumption	Cost [USD/year]
Electricity	1 222 896 $kWh/year$	39 991
Steam	4 578 $tonne/year$	33 462
DEPG (consumption+disposal)	37,45 $m^3/year$	119 258
N_2	161 067 $m^3/year$	74 215
Total		266 926

Table 5.2.3: Income for the DEDPG-scrubbing case.

Product	Production	Income [USD/year]
Methane	2 663 040 $m^3/year$	962 046
CO_2	3054 $tonne/year$	45 812
Total		1 007 858

Table 5.2.4: Fixed costs in the DEPG-scrubbing case.

Fixed cost	Calculated as	Cost [USD]
Property taxes and insurance	2% of fixed capital	94 865
Depreciation	20%	
Annual maintenance	4% of ISBL	104 247
Operator cost (salary)	40 000 USD/operator	40 000
Total		239 112

Results from the investment analysis can be seen in figure 5.2.2. The break even point is in year 9.5, giving a payback time of 9.5 years. The internal rate of return (IRR) was calculated to be 1.07% and the return on investment (ROI) was calculated to 0.59%.

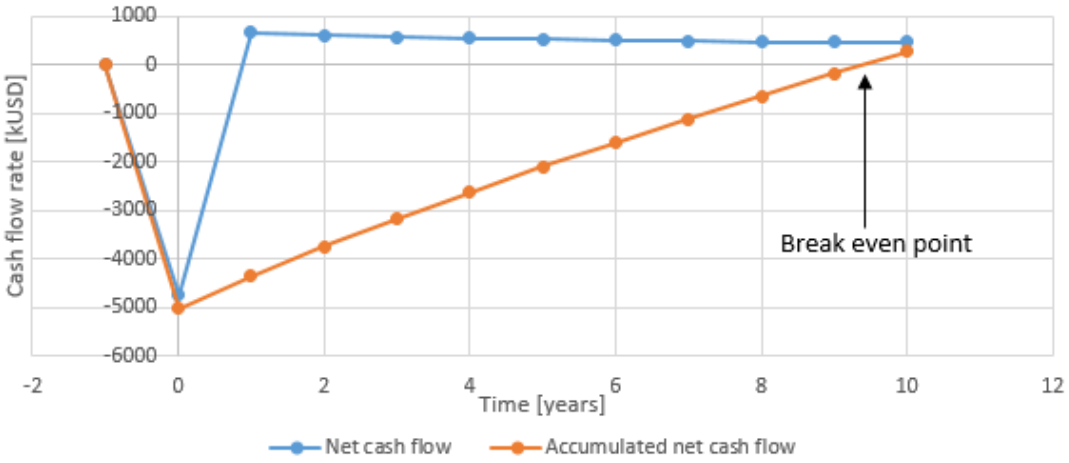

Figure 5.2.2: Net cash flow and accumulated net cash flow for the DEPG-scrubbing plant.

The result of the sensitivity analysis can be seen in figures 5.2.3, 5.2.4, 5.2.5 and 5.2.6. It can be seen that as expected the IRR decreases with increasing investment cost and biogas price, and the IRR increases with increasing methane and CO_2 price. Also in this case the CO_2 price is especially interesting considering the CO_2 stream is not pure, and it can be assumed that the price that can be expected for selling the CO_2 is lower than the price that is used in the investment analysis in this case. This will result in a lower IRR for this case than what is calculated in the investment analysis above. However, also in this case the IRR depend more on the price of methane than on the price of CO_2.

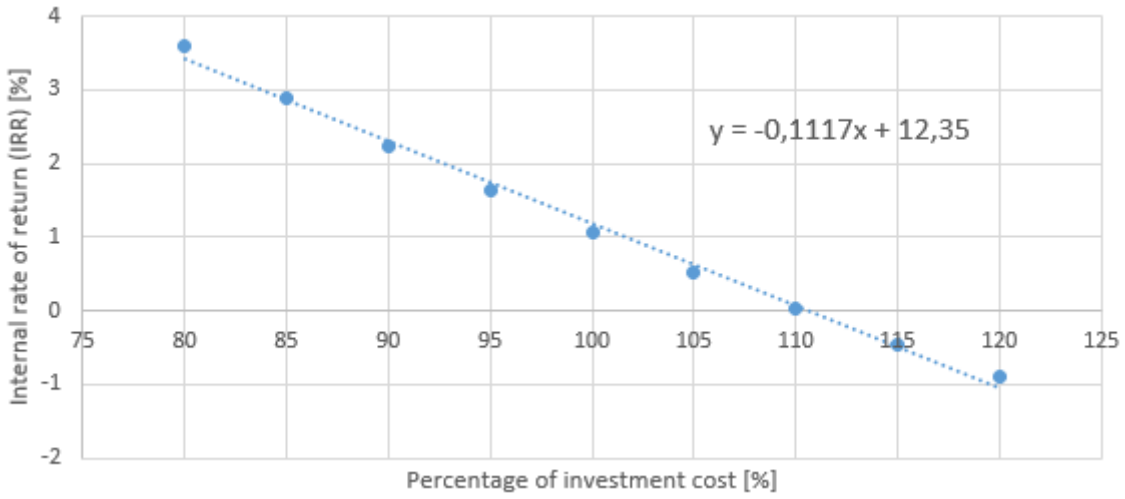

Figure 5.2.3: IRR as a function of the investment cost for the DEPG-scrubbing plant.

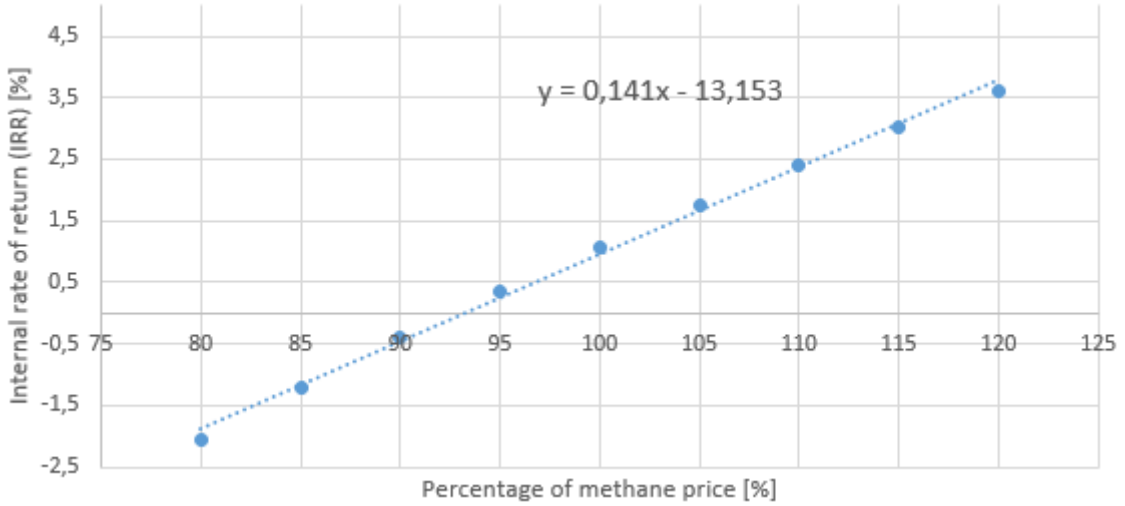

Figure 5.2.4: IRR as a function of methane price for the DEPG-scrubbing plant.

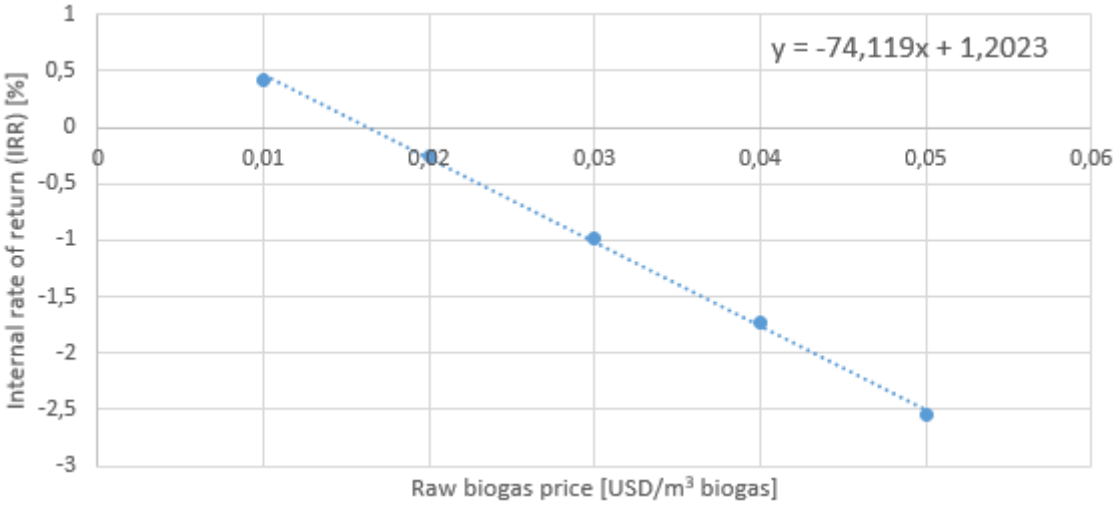

Figure 5.2.5: IRR as a function of biogas price for the DEPG-scrubbing plant.

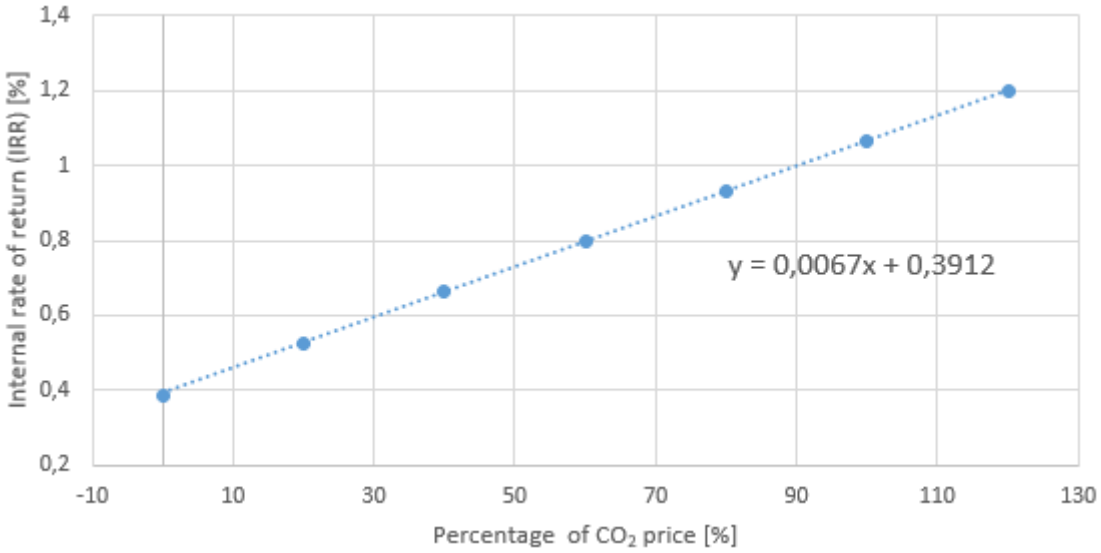

Figure 5.2.6: IRR as a function of CO_2 price for the DEPG-scrubbing plant.

5.3 Amine Scrubbing using MEA

Cost of all equipment is presented in table 5.3.1 and the distribution of the cost is presented in figure 5.3.1. The absorber and desorber cost is the combined cost of the vessel shell and the packing inside. Unlike in water- and DEPG-scrubbing the material used in this process is stainless steel due to the fact that MEA is corrosive. The cost of the coolers is the combined cost of all 11 coolers, the same applies for the combined cost of the 8 compressors and the 9 flash-tanks. The variable costs in the process are given in table 5.3.3. The income of the process is given in table 5.3.2. The variable costs in the process are given in table 5.3.3 and the fixed cost of the process are given in table 5.3.4.

Table 5.3.1: Investment cost for the MEA-scrubbing case.

Equipment	Calculated cost [USD]	ISBL [USD]	Investment cost [USD]
Absorber	61 994	231 858	421 982
Desorber	51 570	192 871	351 025
HX	32 224	120 517	219 341
Coolers	350 447	1 310 672	2 385 423
Flash	56 983	213 115	387 870
Reboiler	35 308	132 054	240 338
Compressors	141 185	528 031	961 017
SUM	729 711	2 729 119	4 966 996

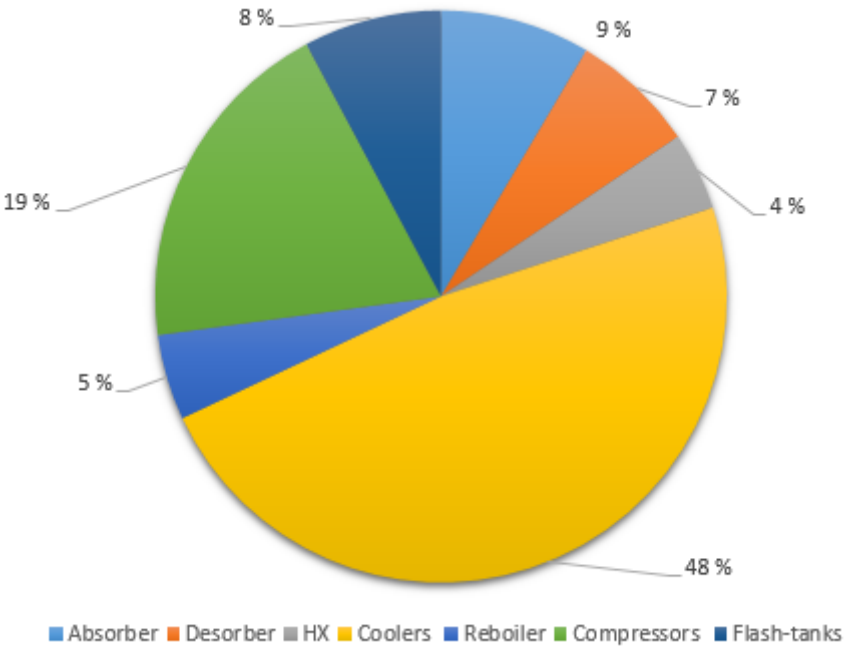

Figure 5.3.1: Distribution of the total equipment cost for MEA-scrubbing plant.

Here, as in the previous cases, it can be observed that all the coolers in the system accounts for the biggest combined equipment cost. The most expensive single unit is the absorber with 9% of the cost. The smallest cost is the cost of the flash-tanks used in the compression-trains.

Table 5.3.2: Income for the MEA-scrubbing case.

Product	Production	Income [USD/year]
Methane	2 813 766 $m^3/year$	1 015 431
CO_2	3048 $tonne/year$	45 720
Total		1 061 151

Table 5.3.3: Variable cost for the MEA-scrubbing case.

Item	Total consumption	Cost [USD/year]
Electricity	853 224 $kWh/year$	27 902
Steam	5 432 $tonne/year$	39 708
Water	2,63 $m^3/year$	4
MEA (consumption+disposal)	1,13 $m^3/year$	3636
Total		71 250

Table 5.3.4: Fixed costs in the MEA-scrubbing case.

Fixed cost	Calculated as	Cost [USD]
Property taxes and insurance	2% of fixed capital	99 340
Depreciation	20%	
Annual maintenance	4% of ISBL	109 165
Operator cost (salary)	40 000 USD/operator	40 000
Total		248 505

The result of the investment analysis can be seen in figure 5.3.2. The payback time for the MEA chemical absorption plant is 7.5 years. The IRR was calculated to 3.05% and the ROI was calculated to 2.94%.

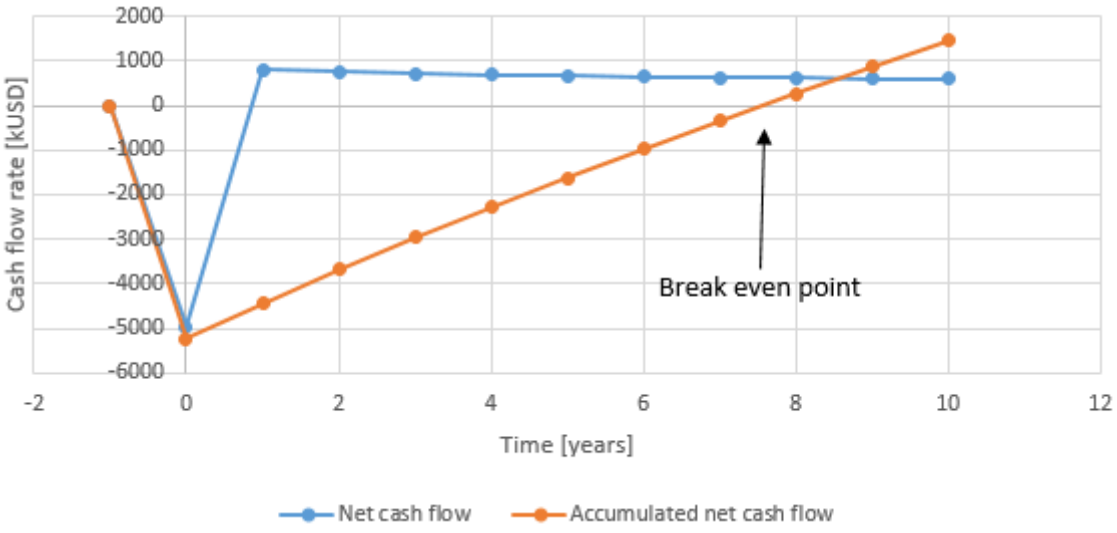

Figure 5.3.2: Net cash flow and accumulated net cash flow for the MEA-scrubbing plant.

Figure 5.3.3, 5.3.5, 5.3.4 and 5.3.6 shows the sensitivity analysis for the MEA chemical absorption case. It can be seen that the IRR decrease with increasing investment cost and biogas price as expected, and the IRR increases with increasing methane and CO_2 sales price as expected.

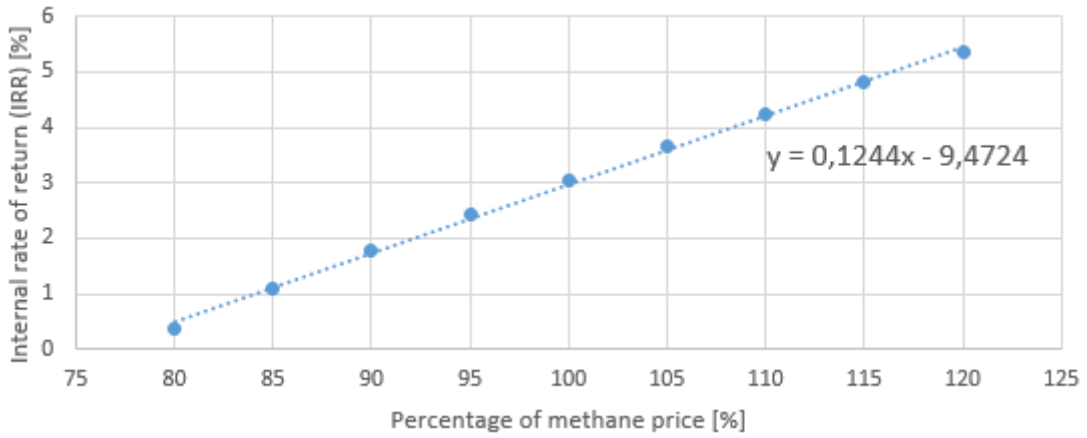

Figure 5.3.3: IRR as a function of methane sales price for the MEA-scrubbing plant.

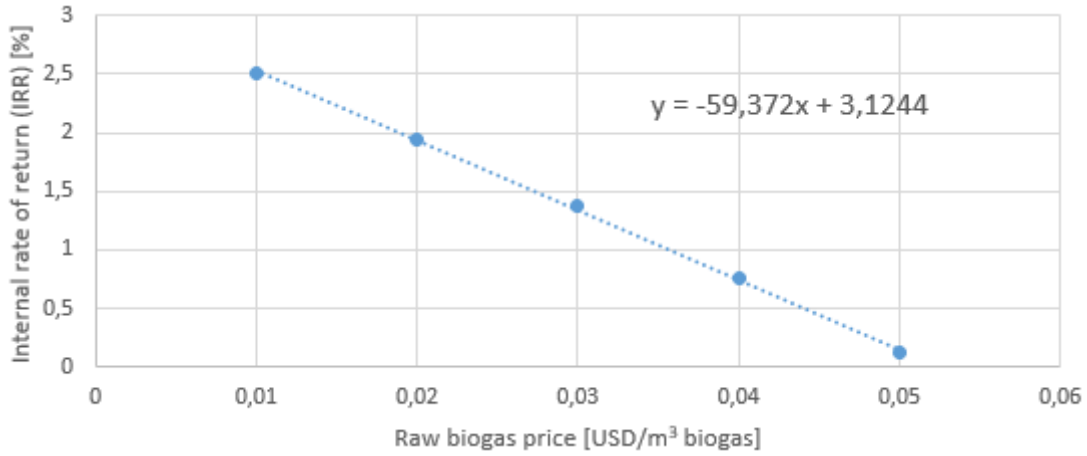

Figure 5.3.4: IRR as a function of biogas price for the MEA-scrubbing plant.

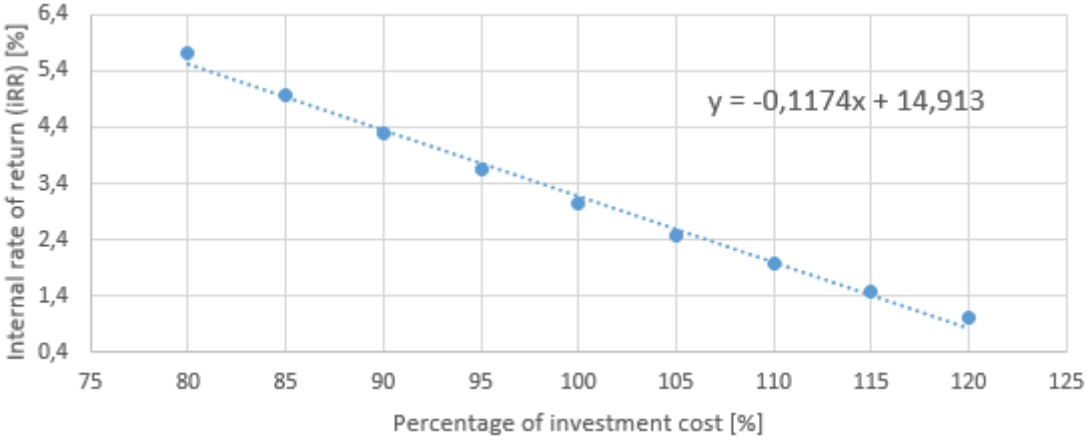

Figure 5.3.5: IRR as a function of investment cost for the MEA-scrubbing plant.

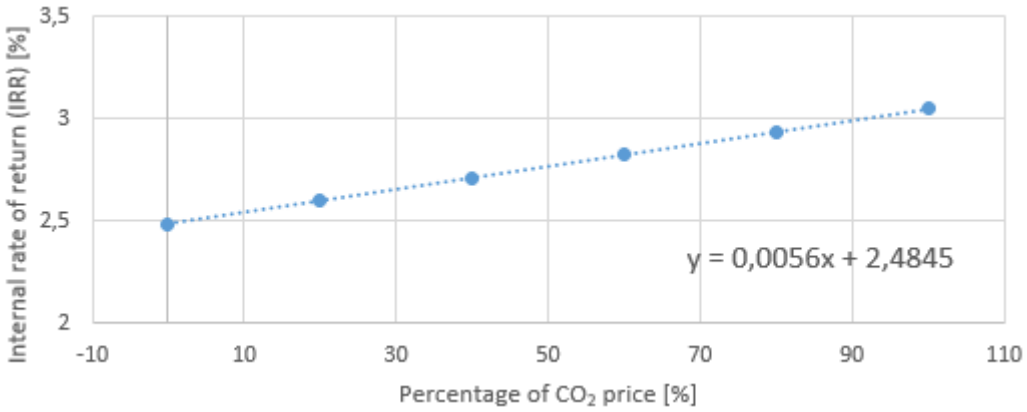

Figure 5.3.6: IRR as a function of CO_2 price for the MEA-scrubbing plant.

6 Comparison

6.1 Simulations

In table 6.1.1 numbers from the three scrubbing technologies are given to easily compare the cases. In this work, the methane purity of 97.5% was set as a goal since that is the purity needed for injection of biomethane into the natural gas grid. It should therefore be remembered that the conclusions from this work would be different if the purity requirement was chosen to be lower for production of biomethane for other applications.

Table 6.1.1: Comparison of the different scrubbing technologies.

	Water-scrubbing	DEPG-scrubbing	MEA-scrubbing
Electricity consumption [kW]	151.2	139.6	97.4
Heat consumption [kW]	870.0	305.9	363.0
Overall power (heat) .[MJ/kg CO_2 removed]	13.0	6.8	6.3
Methane slip [%]	5.0	5.0	0.1
Best L/G [kg/kg]	143	100	9.5

All cases keep within the targets of producing a 97.5% pure methane stream and keep the methane slip below 5%. However the methane slip is at the maximum limit for the two physical absorption processes, while for the amine-scrubbing process it is only 0.1%. This is as explained before because of the fact that with chemical absorption the CO_2 is absorbed through reactions with MEA making the L/G-ratio a lot lower, which again makes the unwanted physical absorption of methane a lot lower. A high methane slip is obviously bad for the economy of the plant, as the methane is what is sold and the main source of income for the plant. However, the methane slip can also have environmental effects if the bi-product stream of CO_2 is released to the atmosphere. The CO_2 is a green-house gas, but methane is a stronger green-house gas than CO_2, so this would contribute more to global warming than to release clean CO_2 gas. Plants would probably have a process where they burn the methane rather than to emit it to the atmosphere, but this would be expensive due to low methane concentration in the gas, and thereby there would be a need for a catalyst to be able to burn the gas.

The CO_2 purity will also become less when the methane slip is high, this can be seen for the water-scrubbing case and the DEPG-scrubbing case. This can result in the CO_2 gas not being able to be used in different scenarios, like CCS. The CO_2 purity of the DEPG-scrubbing process is even worse than for the water-scrubbing case, this is because of the nitrogen stripping gas, which also dilutes the CO_2 stream in addition to methane. As mentioned before

the methane can be burned of the gas, the nitrogen would not be that easy to remove from the gas, so this is an even bigger problem in regards of being able to apply CCS technology.

The electricity consumption is higher for the two physical absorption plants than for the MEA-scrubbing plant. This is because of the need to pressurize the biogas before it enters the absorber as the absorber operates at elevated pressures. The need for a pump to pressurize the solvent in physical absorption cases also adds to the electricity consumption. The MEA-scrubbing simulations needs to be optimized further by finding the optimum reboiler duty. The simulations did not converge for higher L/G-ratios than 9,5 which is chosen as the optimum in this case, and it might be possible to get even lower reboiler duty for this process, making it even more profitable. The steam consumption is a lot higher in the water-scrubbing case than in the other two cases. This is because the reboiler uses a lot of energy heating up large water-streams in the desorber. The DEPG-scrubbing case also has a large solvent stream, but since a nitrogen stream is used to strip the CO_2 from the solvent instead of heat, the steam consumption is not elevated in the same way as in the water-scrubbing case. Stripping with nitrogen is also a possibility for the water-scrubbing case and this would decrease the steam consumption of this process, but the CO_2 stream would be further diluted by nitrogen as for the DEPG-scrubbing.

Another factor for the environment apart from the methane slip is the leakage of chemicals. This can happen both from the DEPG-scrubbing and MEA-scrubbing processes. Tables A.0.2 and A.0.3 show that almost no amount of the chemicals are leaving the system, but with the use of chemicals are are always a risk of biological contamination. For the two factors that is investigated in this work, MEA creates less issues with regards to the environment as the methane slip is low and the CO_2 is not emitted to the atmosphere as CCS technology can be used.

6.2 Economics

A overview of the economics of the different plants are given in table 6.2.1 for easy comparison.

The total investment cost does not vary a lot for the three plants. The DEPG-scrubbing plant is the one with the lowest investment cost, this because the equipment size is smaller than for the water-scrubbing case, and also that the material is cheaper than for the MEA-scrubbing case. It can be seen from figures 5.1.1, 5.2.1 and 5.3.1 that the equipment with the largest cost is all the coolers for the process and compressor trains. The most expensive single piece of equipment is the cross heat-exchanger for the water-scrubbing and the DEPG-scrubbing cases, while this equipment does not contribute so much to the cost in the MEA-scrubbing case. This is due to the fact that the chemical absorption case have a lot

Table 6.2.1: Comparison of the economics of the different scrubbing technologies.

	Water-scrubbing	DEPG-scrubbing	MEA-scrubbing
Methane income	966 834	962 046	1 015 431
CO_2 income	45 764	45 812	45 720
Total income	1 012 598	1 007 858	1 061 151
Utility cost	138 482	73 453	67 610
Chemical cost	87	193 473	3 640
Investment cost	4 997 101	4 743 247	4 966 996
Fixed cost	249 768	239 112	248 505

smaller streams, requiring less energy to be heated. The equipment contributing the least to the cost for the water-scrubbing and DEPG-scrubbing is the pump. For the MEA-scrubbing case the cost is more evenly distributed throughout all the equipment.

Figures 5.1.2, 5.2.2 and 5.3.2 shows the cash flow for the plants. The graph starts in year -1 where all cash flows are at zero since nothing has happened yet. Then in year 0 the cash flow rate curve decreases due to the investment. The cash flow then increases again in year 1 as production starts. As the years go the the cash flow decreases a small amount each year, due to decreasing depreciations.

The payback time is higher and the IRR is lower for the physical absorption processes than it is for the MEA-scrubbing case. The water-scrubbing case has about the same investment cost as the MEA case, but the energy demand of the process increases the variable cost, making it less profitable. The DEPG-scrubbing case has a lower investment cost than both the water- and MEA-scrubbing case, but the higher chemical cost due to the need of large amounts of DEPG and nitrogen increases the variable cost so that the process gets less profitable than the MEA-scrubbing case. Another reason why the MEA-case is more profitable is the higher income due to smaller methane slip, which means there is more methane to sell, thereby increasing the revenue. The low methane slip also means that the CO_2 stream is pure and ready to be sold. In contrast, the two physical absorption plants produce a CO_2 stream that is not pure. This means that the CO_2 might not be salable, meaning that the income of these plants would decrease. The sensitivity analysis of the CO_2 price shows that the IRR would decrease with a decreasing price for the CO_2, making the MEA-case even more profitable compared to the two other processes.

Figures 5.1.6, 5.2.6 and 5.3.6 show that even though the IRR would decrease as the income from CO_2 sales decrease, the change is small. The reason for this is that the CO_2 income is just a small part of the total income of the plants, which is mainly from the sale of methane. This means that even though the CO_2 from the physical absorption cases is not pure, and thereby might not be sold at all, this will not have the biggest effect on the total economy of the plants.

The slope of figures 5.1.4, 5.2.4 and 5.3.3 show that the DEPG-scrubbing case is the most vulnerable to changes in the methane price, but the slope is quite similar for all three cases. It can be seen from the figures that while the MEA-scrubbing case can handle a drop in the methane price down to 80% of the original price, while the physical absorption cases get a negative IRR if the price drops below around 90% of the original price. This shows that the MEA-scrubbing process is the most robust to fluctuations in the gas-price.

Figures 5.1.5, 5.2.5 and 5.3.4 shows the DEPG-scrubbing case is most vulnerable to changes in the biogas price as well, as the slope of the curve is highest for this case. The MEA case is also profitable with a much higher biogas price than the physical absorption methods. They only give a positive IRR up to a price of 0.023-0.025 USD/m^3 biogas, while the MEA chemical absorption case can produce a positive IRR up to a price of over 0.05 USD/m^3 biogas.

Figures 5.1.3, 5.2.3 and 5.3.5 show that a change in the investment cost changes the IRR about the same amount for all three cases. The slope of the curve is the same, but due to the fact that the IRR is lower to begin with for the physical absorption cases, they are more vulnerable to changes in the investment cost. The sensitivity analysis show that an increase in the investment cost of 15% is a maximum for the physical absorption cases. The sensitivity towards change in the investment cost is important as there lies some uncertainty in the calculations of the cost of the equipment. There will probably be some change in this number as the building up starts, and it is important that the budget of the plant can handle this change.

Altogether the DEPG-scrubbing case is the most fragile process with regards to changes in prices for products and raw biogas, and with regards to changes in the total investment cost. On the other hand the MEA-scrubbing case is the most robust.

7 Future Work

Additionally to simulations already preformed, water-scrubbing should be simulated using nitrogen as stripping gas to see if this is a better solution than the one presented in this work. This would decrease the steam consumption in the process, making it more profitable. The cost of nitrogen would increase the cost, so a comparison of these processes would be necessary.

Furthermore, the methane slip of the water-scrubbing case could might be lowered by adding a flash-tank between the absorber and desorber. This could increase income through increased methane streams and increase the purity of the CO_2 stream. This would pose an extra investment cost, but it could increase the profitability of the plant.

Finally, more time should be used to solve the convergence issue in the MEA-scrubbing case at high L/G-ratios. This would tell if the optimum found in these simulations are the true optimum, or if the simulations could be further optimized. This would require extra time not available for this project.

8 Conclusions

Three scrubbing technologies for biogas upgrading, water-scrubbing, DEPG-scrubbing and MEA-scrubbing, are simulated in Aspen Plus v. 10.1 and an economical analysis is conducted. All simulations reach the desired gas quality of 97.5% methane purity and keeps within the maximum methane slip limit of 5%.

The simulations show that the methane slip is higher for the physical absorption processes than for the MEA-scrubbing process, resulting in lower income and more diluted CO_2 for the physical absorption processes. The DEPG-scrubbing case have additional diluted CO_2 stream as the stripping gas also exits together with the CO_2. As CCS requires a pure CO_2 stream this is not an option for the physical absorption processes without purification of the gas, leading to additional costs, or the gas is released to the atmosphere rather than stored. The sensitivity analysis show that the impact of the high methane slip on the economy is mainly the loss of salable methane. The bi-effect that the CO_2 can not be sold does not affect the plants a lot financially. The environmental loss due to methane slip however will be large if the CO_2 is released into the atmosphere. Further, as the chemical loss from the DEPG- and MEA-scrubbing processes are low, this does not seem to be a problem in these cases.

The equipment cost shows that the worst offenders in all cases are the price of coolers for the compressor trains. The compressors for compressing the biogas prior to absorption are not as large a cost as first assumed. The DEPG-scrubbing process is the process with the lowest total investment cost. Nevertheless the payback time is lower and the IRR higher for the MEA-scrubbing case due to increased income, lower energy consumption and lower chemical costs compared to the other processes. The sensitivity analysis also show that the MEA-scrubbing process is the least effected by changes in the prices of products and raw materials as well as changes in the investment cost.

Combined this indicates that the MEA chemical absorption process is the most promising for production of biomethane with this high purity based on this environmental and economical analysis.

References

[1] Australian government, department of the Environment and Energy (01.03.2019) *Greenhouse effect* retrieved from http://www.environment.gov.au/climate-change/climate-science-data/climate-science/greenhouse-effect

[2] Feron, P.H.M. (2016) *Absorption-Based Post-Combustion Capture of Carbon Dioxide, chapter 1 - Introduction*. Woodhead Publishing DOI:10.1016/C2014-0-03382-5

[3] Oreskes, N. (2004) *The Scientific Consensus on Climate Change*. SCIENCE, 306 (5702), 1686. DOI:10.1126/science.1103618

[4] Global CCS institute (02.03.2019) *WHAT IS CCS? CCS is a climate change technology*. retrived from https://www.globalccsinstitute.com/why-ccs/what-is-ccs/

[5] U.S. Energy Information Administration (EIA) (14.09.2017) *EIA projects 28% increase in world energy use by 2040* retrived from https://www.eia.gov/todayinenergy/detail.php?id=32912

[6] Balat, M., Balat, H. (2009) *Biogas as a Renewable Energy Source—A Review*. Energy Sources, Part A, 31(14), 1280-1293. DOI:10.1080/15567030802089565

[7] Angelidaki, I., Treu, L., Panagiotis, T., Luo, G., Campanaro, S., Wenzel, H., Panagiotis, G.K. (2018) *Biogas upgrading and utilization: Current status and perspectives*. Biotechnology Advances, 36(2); 452-466. DOI:10.1016/j.biotechadv.2018.01.011¨

[8] Surendra, K.C., Takara, D., Hashimoto, A.G., Khanal, S.K. (2014) *Biogas as a sustainable energy source for developing countries: Opportunities and challenges*. Renewable and Sustainable Energy Reviews, 31, 846-859. DOI:10.1016/j.rser.2013.12.015

[9] Muñoz, R., Meier, L., Diaz, I., Jeison, D. (2015) *A review on the state-of-the-art of physical/chemical and biological technologies for biogas upgrading*. Environmental Science and Bio/Technology, 14; 727-759. DOI:10.1007/s11157-015-9379-1

[10] Petersson, A., Wellinger, A. (2009) *Biogas Upgrading Technologies – Developments and Innovations*. IEA Bioenergy Task 37-Energy FromBiogas and Landfill Gas. 37.

[11] IEA Bioenergy (2015) *Solrød Biogas – TOWARDS A CIRCULAR ECONOMY*. BIOGAS IN SOCIETY A Case Story from IEA BIOENERGY TASK 37 “Energy from Biogas”

[12] IEA Bioenergy (2015) *RINGKØBING-SKJERN, DENMARK – DECENTRALISED BIOGAS NETWORK MODEL*. BIOGAS IN SOCIETY A Case Story from IEA BIOENERGY TASK 37 “Energy from Biogas”

[13] Ryckebosch, E., Drouillon, M., Vervaeren, H. (2011) *Techniques for transformation of biogas to biomethane*. Biomass and Bioenergy, 35(5); 1633-1645. DOI:10.1016/j.biombioe.2011.02.033

[14] Sahota, S., Shah, G., Ghosh, P., Kapoor, R., Senggupta, S., Singh, P., Vijay, V., Sahay, A., Vijay, V.K., Thakur, I.S. (2018) *Review of trends in biogas upgrading technologies and future perspectives*. Bioresource Technology Reports, 1; 79-88. DOI:10.1016/j.biteb.2018.01.002

[15] Sun, Q., Li, H., Yan, J., Liu, L., Yu, Z., Yu, X. (2015) *Selection of appropriate biogas upgrading technology-a review of biogas cleaning, upgrading and utilisation.* Renewable and Sustainable Energy Reviews 51; 521-532. DOI:10.1016/j.rser.2015.06.029

[16] Goto,K., Okabe, H., Shimizu, S., Onoda, M., Fujioka, Y. (2009) *Evaluation method of novel absorbents for CO2 capture.* Energy Procedia 1(1); 1083-1089 DOI:10.1016/j.egypro.2009.01.143

[17] Herzog, H., Meldon, J., Hatton, A. (2009) *Advanced Post-Combustion CO2 Capture.* Prepared for the Clean Air Task Force

[18] Feron, P.H.M. (2016) *Absorption-Based Post-Combustion Capture of Carbon Dioxide, chapter 3 - Conventional amine scrubbing for CO2 capture.* Woodhead Publishing DOI:10.1016/C2014-0-03382-5

[19] Zhang, Y., Chen, H., Chen, C., Plaza, J.M., Dugas, R., Rochelle, G.T. (2009) *Rate-Based Process Modeling Study of CO_2 Capture with Aqueous Monoethanolamine Solution.* Industrial & Engineering Chemistry Research, 48(20), 9233–9246. DOI:10.1021/ie900068k

[20] Cozma, P., Wukovits, W., Mamaliga, I., Friedl, A., Gavrilescu, M. (2014) *Modeling and simulation of high pressure water scrubbing technology applied for biogas upgrading.* Clean Technologies and Environmental Policy, 17(2). DOI: 10.1007/s10098-014-0787-7

[21] Cozma, P., Wukovits, W., Mamaliga, I., Friedl, A., Gavrilescu, M. (2013) *Analysis and modelling of the solubility of biogas components in water for physical absorption processes.* Environmental Engineering and Management Journal, 12(1); 147-162. DOI:10.30638/eemj.2013.017

[22] Carroll, J.J., Slupsky J.D., Mather, A.E. (1991) *The Solubility of Carbon Dioxide in Water at Low Pressure.* Journal of Physical and Chemical Reference Data, 20: 1201-1209. DOI: 10.1063/1.555900

[23] Zawisza, A., Malesinska, B. (1981) *Solubility of carbon dioxide in liquid water and of water in gaseous carbon dioxide in the range 0.2-5 MPa and at temperatures up to 473 K.* Journal of Chemical & Engineering Data , 26 (4): 388-391. DOI: 10.1021/je00026a012

[24] Aspen Technology (2001) *Physical property methods and models 11.1*

[25] Valtz, A., Chapoy, A., Coquelet, C., Paricaud, P., Richon, D. (2004). *Vapour-liquid equilibria in the carbon dioxide-water system, measurement and modelling from 278.2 to 318.2K.* Fluid Phase Equilibria, 226: 333-344. DOI: 10.1016/j.fluid.2004.10.013

[26] Chapoy, A., Mohammadi, A. H., Richon, D., Tohidi, B. (2004). *Gas solubility measurement and modeling for methane–water and methane–ethane–n-butane–water systems at low temperature conditions.* Fluid Phase Equilibria, 220(1); 111–119. DOI:10.1016/j.fluid.2004.02.010

[27] Gainar, I., Anitescu, G. (1995) *The solubility of CO_2, N_2 and H_2 in a mixture of dimethylether polyethylene glycols at higher pressures.* Fluid Phase Equilibria, 109(2): 281-289. DOI: 10.1016/0378-3812(95)02729-X

[28] Rayer, A.V., Henni, A., Tontiwachwuthikul, P. (2012) *High pressure physical solubility of*

carbon dioxide (CO_2) in mixed polyethylene glycol dimethyl ethers (Genosorb 1753). The Canadian Journal of Chemical Engineering, 90(3): 576-583. DOI:10.1002/cjce.20615

[29] Henni, A., Tontiwashwuthikul, P., Chakma (2006) *Solubility Study of Methane and Ethane in Promising Physical Solvents for Natural Gas Sweetening Operations*. Journal of Chemical & Engineering Data, 51 (1): 64–67. DOI:10.1021/je050172h

[30] U.E. Aronu et al. (2011) *Solubility of CO2 in 15, 30, 45 and 60 mass% MEA from 40 to 120°C and model representation using the extended UNIQUAC fremework*. Chemical Engineering Science 66(24): 6393–6406. DOI:10.1016/j.ces.2011.08.042

[31] Lee, J. I., Otto, F. D. and Mather, A. E. (1976) *Equilibrium Between Carbon Dioxide and Aqueous Monoethanolamine Solutions*. Journal of Applied Chemistry, 26: 541-549. DOI:10.1002/jctb.5020260177

[32] Bhatia, S.C. (2014) *Advanced Renewable Energy Systems 19 - Cogeneration*. Woodhead Publishing India. 490-508 DOI:10.1016/B978-1-78242-269-3.50019-X

[33] Burr, B., Liddon, L. *A COMPARISON OF PHYSICAL SOLVENTS FOR ACID GAS REMOVAL* Bryan Research & Engineering, Inc, Bryan, Texas, U.S.A.

[34] Sinnott, R., Towler, G., (2009) *Chemical engineering design* fifth edition. Butterworth-Heinemann, Elsevier.

[35] Rotunno, P., Lanzini, A., Leone, P. (2017) *Energy and economic analysis of a water scrubbing based biogas upgrading process for biomethane injection into the gas grid or use as transportation fuel*. Renewable Energy 102(B); 417-432 DOI:10.1016/j.renene.2016.10.062

[36] NORDPOOL (30.12.2018) *Day-ahead prices* https://www.nordpoolgroup.com/Market-data1/Dayahead/Area-Prices/NO/Daily1/?view=table

[37] Oslo kommune (01.01.2019) *Vann- og avløpsgebyrer* https://www.oslo.kommune.no/vann-og-avlop/priser-beregninger-og-vannmaler/vann-og-avlopsgebyrer/#gref

[38] Intratec Solutions (2017) *Monoethanolamine Price History* https://www.intratec.us/chemical-markets/monoethanolamine-price

[39] Echemi Technology Co. (08.05.2019) *Polyethylene Glycol Price Analysis* https://www.echemi.com/productsInformation/pd20150901277-polyethylene-glycol.html

[40] Purity (2017) *Costs of nitrogen gas – how much should you be paying?* https://puritygas.ca/nitrogen-gas-costs/

[41] DNV GL maitime (2019) *Current price development oil and gas* https://www.dnvgl.com/maritime/lng/current-price-development-oil-and-gas.html

[42] Global CCS institute, Chemical Economics Handbook 2010 (03.2010) *The CO2 market* https://hub.globalccsinstitute.com/publications/accelerating-uptake-ccs-industrial-use-captured-carbon-dioxide/2-co2-market#fn_p02_001

[43] Jenkins, S., 20.03.2019 *2019 CEPCI UPDATES: JANUARY (PRELIM.)*

AND DECEMBER 2018 (FINAL) https://www.chemengonline.com/2019-cepci-updates-january-prelim-and-december-2018-final/

[44] Seider, W.D., Seader, J.D., Lewin, D.R., Widagdo, S. (2009) *PRODUCT AND PROCESS DESIGN PRINCIPLES Synthesis, Analysis, and Evaluation* third edition. John Wiley & Sons, Inc.

[45] Woods, D.R. (2007) *Rules of Thumb in Engineering Practice Appendix D: Capital Cost Guidelines* DOI:10.1002/9783527611119.app4

Appendices

A Stream Data

In tables A.0.1, A.0.2 and A.0.3 all stream data for all three processes are given. The temperature, pressure, moleflow, molar vapour fraction and the mole-fractions of all components in the stream are given.

Table A.0.1: Stream data for all streams in the water-scrubbing simulations.

Streams	T [C]	P [bar]	Moleflow [kmol/h]	Vapor fraction [mole/mole]	CH_4	CO_2	H_2O
Biogas	30	1	21.43	1.00	0.574	0.383	0.043
Methane	30	80	11.98	1.00	**0.975**	0.024	0.001
CO_2	30	80	8.56	1.00	0.073	**0.925**	0.002
1	145	3	21.43	1.00	0.574	0.383	0.043
2	30	3	21.43	0.97	0.574	0.383	0.043
3	30	3	20.80	1.00	0.592	0.394	0.014
4	149	10	20.80	1.00	0.592	0.394	0.014
5	30	10	20.80	0.99	0.592	0.394	0.014
6	30	3	0.63	0.00	4.1E-05	6.5E-04	0.999
7	30	10	0.20	0.00	1.3E-04	0.002	0.998
Absorber-in	30	10	20.61	1.00	0.597	0.398	0.005
Lean-in	30	10	4506.91	0.00	5.7E-12	5.6E-05	0.999
Rich-out	30	10	4515.48	0.00	1.4E-4	0.002	0.998
Rich-in	83	10	4515.48	0.00	1.4E-4	0.002	0.998
Lean-out	91	1	4506.91	0.00	5.7E-12	5.6E-05	0.999
Lean-out2	91	10	4506.91	0.00	5.7E-12	5.6E-05	0.999
Lean-out3	38	10	4506.91	0.00	5.7E-12	5.6E-05	0.999
Gasout	30	10	12.02	1.00	0.972	0.023	0.005
8	149	32	12.02	1.00	0.972	0.023	0.005
9	30	32	12.02	1.00	0.972	0.023	0.005
10	30	32	11.98	1.00	0.975	0.023	0.002
11	124	80	11.98	1.00	0.975	0.023	0.002
12	30	80	11.98	1.00	0.975	0.023	0.002
13	30	32	0.03	0.00	6.4E-04	3.4E-04	0.999
14	30	80	0.01	0.00	0.001	6.4E-04	0.998
15	82	1	17.35	1.00	0.036	0.456	0.507
16	30	1	17.35	0.52	0.036	0.456	0.507
17	30	1	8.42	0.00	1.6E-06	4.8E-04	0.999
18	30	1	8.93	1.00	0.070	0.887	0.043
19	140	3	8.93	1.00	0.070	0.887	0.043
20	30	3	9.93	0.97	0.070	0.887	0.043
21	30	3	8.67	1.00	0.072	0.913	0.015
22	30	3	0.26	0.00	4.9E-06	0.001	0.999
23	140	9	8.67	1.00	0.072	0.913	0.015
24	30	9	8.67	0.99	0.072	0.913	0.015
25	30	9	8.59	1.00	0.073	0.922	0.005
26	30	9	0.08	0.00	1.4E-05	0.004	0.996
27	141	27	8.59	1.00	0.073	0.922	0.005
28	30	27	8.59	1.00	0.073	0.922	0.005
29	30	27	8.56	1.00	0.073	0.925	0.002
30	30	27	0.03	0.00	4.1E-05	0.011	0.989
31	140	80	8.56	1.00	0.073	0.925	0.002
32	30	80	8.56	1.00	0.073	0.925	0.002
33	30	80	5.1E-05	0.00	1.3E-04	0.019	0.908

Table A.0.2: Streamdata for the DEPG-scrubbing simulations.

Streams	T [°C]	P [bar]	Vapor fraction [mole/mole]	Mole Flows [kmol/hr]	DEPG	CO_2	H_2O	N_2	CH_4
Biogas	30	1	1.00	21.43	0	0.383	0.042	0	0.575
Abs-in	20	8	1.00	25.30	5.0E-06	0.430	0.003	3.0E-05	0.567
Leanin	20	8	0.00	208.47	0.956	0.004	0.040	1.1E-04	7.8E-06
Richout	22	8	0.00	221.49	0.900	0.0518	0.038	3.6E-06	0.011
Richout2	72	8	0.00	221.49	0.900	0.0518	0.038	3.6E-06	0.011
Richout3	72	6	0.00	216.77	0.920	0.041	0.038	1.8E-07	0.002
Richin	80	6	0.00	216.77	0.920	0.041	0.038	1.8E-07	0.002
Nitrogen	20	1	1.00	0.75	0	0	0	1.000	0
Leanout	79	1	0.00	208.46	0.956	0.004	0.039	1.1E-04	7.8E-06
Leanout2	80	8	0.00	208.46	0.956	0.004	0.039	1.1E-04	7.8E-06
Leanout3	30	8	0.00	208.46	0.956	0.004	0.039	1.1E-04	7.8E-06
Methane recycle	72	6	1.00	4.72	2.7E-05	0.566	0.001	1.6E-04	0.433
Methane recycle2	102	8	1.00	4.72	2.7E-05	0.566	0.001	1.6E-04	0.433
Methane recycle3	20	8	1.00	4.72	2.7E-05	0.566	0.001	1.6E-04	0.433
1	142	3	1.00	21.43	0	0.383	0.042	0	0.575
2	30	3	0.97	21.43	0	0.383	0.042	0	0.575
3	30	3	1.00	20.83	0	0.394	0.015	0	0.591
4	30	3	0.00	0.60	0	3.8E-04	1.000	0	3.8E-05
5	133	8	1.00	20.83	0	0.394	0.015	0	0.591
6	20	8	0.99	20.83	0	0.394	0.015	0	0.591
7	20	8	0.00	0.25	0	0.001	0.999	0	9.4E-05
8	20	8	1.00	20.58	0	0.399	0.003	0	0.598
Gasout	20	8	1.00	12.28	7.2E-08	0.023	2.5E-04	0.002	0.975
9	145	27	1.00	12.28	7.2E-08	0.023	2.5E-04	0.002	0.975
10	30	27	1.00	12.28	7.2E-08	0.023	2.5E-04	0.002	0.975
11	144	80	1.00	12.28	7.2E-08	0.023	2.5E-04	0.002	0.975
Methane	30	80	1.00	12.28	7.2E-08	0.023	2.5E-04	0.002	**0.975**
12	80	1	1.00	9.06	2.9E-04	0.874	0.008	0.080	0.037
13	30	1	0.99	9.06	2.9E-04	0.874	0.008	0.080	0.037
14	30	1	1.00	9.06	1.5E-06	0.875	0.008	0.080	0.037
15	30	1	0.00	0.003	0.854	0.019	0.127	3.1E-05	4.7E-05
16	147	3	1.00	9.06	1.5E-06	0.875	0.008	0.080	0.037
17	30	3	1.00	9.06	1.5E-06	0.875	0.008	0.080	0.037
18	30	3	1.00	9.06	3.8E-07	0.875	0.008	0.080	0.037
19	30	3	0.00	1.6E-05	0.598	0.040	0.361	6.2E-05	9.4E-05
20	142	9	1.00	9.06	3.8E-07	0.875	0.008	0.080	0.037
21	30	9	0.99	9.06	3.8E-07	0.875	0.008	0.080	0.037
22	30	9	1.00	9.03	9.7E-08	0.877	0.005	0.080	0.037
23	30	9	0.00	0.03	1.0E-04	0.003	0.997	4.1E-06	7.2E-06
24	142	27	1.00	9.03	9.7E-08	0.877	0.005	0.080	0.037
25	30	27	0.99	9.03	9.7E-08	0.877	0.005	0.080	0.037
26	30	27	1.00	9.00	1.9E-08	0.880	0.002	0.081	0.037
27	30	27	0.00	0.03	2.4E-05	0.007	0.993	1.3E-05	2.2E-05
28	142	80	1.00	9.00	1.9E-08	0.880	0.002	0.081	0.037
CO_2	30	80	1.00	9.00	1.9E-08	**0.880**	0.002	0.081	0.037

Table A.0.3: Stream data for all streams in the MEA-scrubbing simulations.

Streams	T [C]	P [bar]	Moleflow [kmol/h]	Vapor fraction [mole/mole]	CH_4	CO_2	MEA	H_2O	H_3O^+	OH^-	HCO_3^-	CO_3^{2-}	MEAH+	MEACOO-
Biogas	30	1	21.43	1.00	0.574	0.383	0	0.043	0	0	0	0	0	0
Methane	30	80	12.61	1.00	**0.975**	0.024	0	9.2E-04	0	0	0	0	0	0
CO_2	30	80	7.92	1.00	0.002	**0.998**	0	9.4E-04	0	0	0	0	0	0
Gas-out	61	1	15.26	1.00	0.806	0.020	6.5E-05	0.174	0	0	0	0	0	0
Rich-out	58	1	228.17	0.00	5.4E-05	3.5E-05	0.006	0.873	3.6E-10	4.0E-07	0.014	0.001	0.061	0.045
Rich-in	85	1	229.63	0.01	5.4E-05	0.006	0.015	0.871	5.1E-10	9.7E-07	0.010	5.3E-04	0.054	0.043
Lean-out	102	1	227.79	0.00	0	7.2E-06	0.063	0.886	1.2E-10	4.3E-06	0.002	1.6E-04	0.026	0.024
Lean-out2	66	1	227.79	0.00	0	4.5E-07	0.062	0.887	2.0E-11	4.7E-06	7.4E-04	3.2E-04	0.026	0.025
Lean-in	30	1	227.79	0.00	0	2.0E-08	0.061	0.887	2.1E-12	4.1E-06	2.5E-04	5.7E-04	0.026	0.025
1	30	1	15.25	0.86	0.806	0.020	2.1E-06	0.174	4.1E-11	2.9E-09	6.1E-05	3.5E-07	6.2E-05	8.9E-07
2	30	1	2.09	0.00	2.2E-05	1.2E-05	1.5E-05	0.999	3.0E-10	2.1E-08	4.4E-04	2.6E-06	4.5E-04	6.5E-06
3	30	1	13.16	1.00	0.934	0.023	2.7E-09	0.043	0	0	0	0	0	0
4	144	3	13.16	1.00	0.934	0.023	2.7E-09	0.043	0	0	0	0	0	0
5	30	3	13.16	0.97	0.934	0.023	5.5E-14	0.043	1.4E-08	2.7E-13	1.7E-08	3.2E-14	2.7E-09	3.1E-17
6	30	3	0.38	0.00	6.5E-05	3.8E-05	1.9E-12	0.999	5.0E-07	9.4E-12	5.9E-07	1.1E-12	9.4E-08	1.1E-15
7	30	3	12.78	1.00	0.962	0.024	1.2E-16	0.014	0	0	0	0	0	0
8	144	9	12.78	1.00	0.962	0.024	1.2E-16	0.014	0	0	0	0	0	0
9	30	9	12.78	0.99	0.962	0.024	0	0.014	8.9E-09	4.8E-14	8.9E-09	9.1E-15	0	0
10	30	9	0.12	0.00	1.9E-04	1.1E-04	0	0.999	9.4E-07	5.1E-12	9.4E-07	9.5E-13	0	0
11	30	9	12.66	1.00	0.971	0.024	0	0.005	0	0	0	0	0	0
12	144	27	12.66	1.00	0.971	0.0238	0	0.005	0	0	0	0	0	0
13	30	27	12.66	0.99	0.971	0.024	0	0.005	5.0E-09	9.7E-15	5.0E-09	3.1E-15	0	0
14	30	27	0.04	0.00	5.5E-04	3.0E-04	0	0.999	1.6E-06	3.1E-12	1.6E-06	9.8E-13	0	0
15	30	27	12.62	1.00	0.974	0.024	0	0.002	0	0	0	0	0	0
16	144	80	12.62	1.00	0.974	0.024	0	0.002	0	0	0	0	0	0
17	30	80	12.62	1.00	0.974	0.024	0	0.002	2.4E-09	2.0E-15	2.4E-09	1.0E-15	0	0
18	30	80	0.01	0.00	0.001	7.0E-04	0	0.998	2.5E-06	2.1E-12	2.5E-06	1.0E-12	0	0
19	87	1	18.73	1.00	6.6E-04	0.422	2.9E-04	0.577	0	0	0	0	0	0
20	30	1	18.72	0.44	6.6E-04	0.422	2.7E-07	0.576	6.0E-09	3.36E-10	2.90E-04	4.78E-08	2.90E-04	1.35E-07
21	30	1	10.45	0.00	3.53E-08	5.07E-04	4.86E-07	0.998	1.07E-08	6.0E-10	5.2E-04	8.6E-08	5.2E-04	2.4e-07
22	30	3	8.27	1.00	0.002	0.956	8.6E-11	0.043	0	0	0	0	0	0
23	140	3	8.27	1.00	0.002	0.956	8.6e-11	0.043	0	0	0	0	0	0
24	30	3	8.27	0.97	0.002	0.956	2.5E-16	0.043	1.0E-07	3.9E-14	1.0E-07	2.8E-14	8.6E-11	8.3E-19
25	30	3	8.03	1.00	0.002	0.984	5.3E-19	0.014	0	0	0	0	0	0
26	30	3	0.24	0.00	1.0E-07	0.002	8.6E-15	0.99	3.5E-6	1.3E-12	3.5E-6	9.7E-13	3.0E-09	2.9E-17
27	140	9	8.03	1.00	0.002	0.984	5.3E-19	0.014	0	0	0	0	0	0
28	30	9	8.03	0.99	0.002	0.984	0	0.014	5.8E-08	7.5E-15	5.8E-06	9.4E-15	0	0
29	30	9	7.95	1.00	0.002	0.993	0	0.005	0	0	0	0	0	0
30	30	9	0.08	0.00	3.1E-7	0.005	0	0.995	6.0E-06	7.9E-13	6.0E-06	9.9E-13	0	0
31	141	27	7.95	1.00	0.002	0.993	0	0.005	0	0	0	0	0	0
32	30	27	7.95	0.99	0.002	0.993	0	0.005	3.1E-08	1.5E-15	3.1E-08	3.2E-15	0	0
33	30	27	7.93	1.00	0.002	0.996	0	0.002	0	0	0	0	0	0
34	30	27	0.03	0.00	9.2E-7	0.012	0	0.988	9.9E-06	4.8E-13	9.9E-06	1.0E-12	0	0
35	141	80	7.93	1.00	0.002	0.996	0	0.002	0	0	0	0	0	0
36	30	80	7.93	1.00	0.002	0.996	0	0.002	1.5E-08	3.2E-16	1.5E-08	1.0E-15	0	0
37	30	80	0.01	0.00	2.7E-6	0.027	0	0.973	1.5E-05	3.2E-13	1.5E-05	1.0E-12	0	0

B Equipment Cost

Constants and unit if size for equations 5.0.1 and 5.0.2 for all equipment are given in tables B.0.1 and B.0.2.

Table B.0.1: Cost equations for different equipment.

Equipment	S	A	B	n
Absorber/Desorber	kg	10 000	29	0,85
Packing	m^3	-	6 900	1,00
Heat exchanger	m^2	24 000	46	1,20
Reboiler	m^2	25 000	340	0,90
Pump	L/s	6 900	206	0,90

Table B.0.2: Cost equations for different equipment.

Equipment	A	K_1	K_2	K_3
Compressor	kW	5,0355	-0,8002	0,8253
Flash tank	m^3	3,4974	0,4485	0,1074

The cost of the equipment was calculated for prices in 2007 and 2001, and the cost for 2018 was calculated using equation B.0.1. The CEPCI for 2018 was obtained from [43], the CEPCI for 2007 was obtained from [34] and the CEPCI for 2001 was obtained from [35].

$$\text{Cost B} = \text{Cost A}\frac{\text{CEPCI B}}{\text{CEPCI A}} \tag{B.0.1}$$

The ISBL cost was calculated using the factorial method, shown in equation B.0.2 [34].

$$C = \sum_{i=1}^{i=M} C_{e,i,CS}[(1+f_p)f_m + (f_{er}+f_{el}+f_i+f_c+f_s+f_l)] \tag{B.0.2}$$

The total investment cost (fixed capital cost) was calculated using equation B.0.3 [34].

$$C_{FC} = C(1+OS)(1+D\&E+X) \tag{B.0.3}$$

B.1 Absorber and Desorber

The cost of the absorber and desorber was calculated using the shell mass of the column. This was calculated using equation B.1.1. D_c is the diameter of the column, L_c the length of

the column, t_w is the wall thickness and ρ is the density of the metal. The density of carbon steel used is 7850 kg/m^3 while the density for stainless steel is 8000 kg/m^3.

$$\text{Shell mass} = \pi D_c L_c t_w \rho \tag{B.1.1}$$

The diameter of the columns was found in the simulations in Aspen. The length was found by equation B.1.2 where h equals the height found in the simulations and additional 1,2m is added at the top and at the bottom to make room for piping.

$$L_c = h + 1,2 + 1,2 \tag{B.1.2}$$

The wall thickness was found by using equation B.1.3. P_d is the design pressure of the column, which is assumed to be 10% above normal operation pressure. S is the maximum allowable stress, found in [44] to be 15000 psi (ca. 1000 bar) and E is the fractional weld efficiency assumed to be 0,85.

$$t_w = \frac{P_d D_c}{2SE + 1,2P_d} \tag{B.1.3}$$

For low pressures the wall thickness calculated from the equation above might be to small to give sufficient rigidity to vessels. In this case the thickness from table B.1.1 should be used [44].

Table B.1.1: Minimum wall thickness [44]

Vessel diameter [m]	Minimum wall thickness [m]
Up to 1,22	0,0064
1,22-1,83	0,0079
1,83-2,44	0,0095
2,44-3,05	0,0111

B.2 Separators

The flahs tenks was too small for the cost-equations in [34] to be used, so a different cost equation from [35] was used. The volume of the tanks was needed. The volume of the flash-tank was then calculated as the volume of a cylinder.

The diameter of the separators was calculated using equation B.2.1, where V_v is the vapour volumetric flowrate and u_s is the settling velocity. u_s is calculated by equation B.2.2 and B.2.3 and the vapour volumetric flowrate is exrtracted from the simulations.

$$D_c = \sqrt{\frac{4V_v}{\pi u_s}} \tag{B.2.1}$$

$$u_t = 0,07(\frac{\rho_L - \rho_v}{\rho_v})^{0,5} \tag{B.2.2}$$

$$u_s = 0,15u_t \tag{B.2.3}$$

The height of the separator is calculated using equation B.2.4 where h_v is liquid depth required. The liquid depth was calculated using equation B.2.5. The vessel cross-sectional area was calculated using the diameter and the volume hold up was calculated using equation B.2.6 and a hold up time of 10 min was assumed. The liquid volumetric flow rate was extracted from the simulations.

$$L_c = h_v + D_c + \frac{D_c}{2} + 0,4 \tag{B.2.4}$$

$$h_v = \frac{\text{Volume hold up}}{\text{vessel cross-sectional area}} \tag{B.2.5}$$

$$\text{Volume hold up} = \text{Liquid volumetric flow rate} * \text{Hold up time} \tag{B.2.6}$$

This cost equation calculates the cost for the vessel at ambient pressure, to take into account the pressure the price was multiplied with a pressure factor, these factors are given in table B.2.1 [45].

Table B.2.1: Pressure factors for calculating cost of flash-tanks.

Pressure [bar]	Factor
Up to 3,4	1,00
3,4 - 21,0	1,25
21,0 - 40,0	2,40
40,0 - 100,0	8,20

B.3 Packing Material

To calculate the cost of the packing the volume of the packing was needed. This was done using equation B.3.1, calculating the volume of a cylinder. The height and radius of the

columns was found in the simulations in Aspen Plus.

$$V = \pi r^2 h \tag{B.3.1}$$

B.4 Heat-exchanger

The cost of the heat-exchangers are calculated using the area of the exchangers. The area of the heat-exchangers are calculated using equation B.4.1 where A is the area and U is the overall heat transfer coefficient. The UA value is collected from the simulations and the U is found in [34]. The values used for the U are given in table B.4.2.

$$A = \frac{UA}{U} \tag{B.4.1}$$

Table B.4.1: Heat transfer coefficients.

Hot fluid	Cold fluid	U $[W/m^2°C]$
Water	Water	800-1500
Organic solvent	Organic solvent	100-300
Gases	Water	20-300
Steam	Water	1500-4000
Steam	Organic solvent	500-1000
Organic solvent	Water	250-750

Table B.4.2: Heat transfer coefficients used.

Hot fluid	Cold fluid	U $[W/m^2°C]$
Water	Water	800
Gases	Water	20
Steam	Water	1500
30% MEA	Water	500
30% MEA	30% MEA	500
Steam	30% MEA	1000
DEPG	DEPG	300
Steam	DEPG	600
DEPG	Water	500

The reboiler was calculated as a steam-water heat-exchanger, using equation B.4.2 to calculate the area. ΔT_{min} is calculated using equation B.4.3 and Q is the heat requirement from the simulations. The steam used in the reboiler is assumed to be at 120 °C.

$$A = \frac{Q}{U\Delta T_{min}} \tag{B.4.2}$$

$$\Delta T_{min} = \frac{\Delta T_1 - \Delta T_2}{ln(\Delta T_1 / \Delta T_2)} \tag{B.4.3}$$

B.5 Pressure Changers

The cost of the pumps was calculated using the flow through the pumps which was directly extracted from the simulations.

The compressors in the simulations are small and therefore the cost-calculations given in [34] could not be used. A different cost equation, from [35] was used, and the cost was calculated using the power needed in the compressors, obtained directly from the simulations.

C Investment Analysis

For the investment analysis the IRR and the ROI was calculated. The IRR was calculated using equation C.0.1 [34], where t is the lifetime of the project in years, CF_n is the cash flow in year n and i is the interest rate. The IRR is the value of i that gives a NPV equal to zero.

$$NPV = \sum_{n=1}^{n=t} \frac{CF_n}{(1+i)^n} \tag{C.0.1}$$

The ROI was calculated as a average over the whole project using equation C.0.2 [34].

$$ROI = \frac{\text{cumulative net profit}}{\text{plant life} * \text{initial investment}} * 100\% \tag{C.0.2}$$

NTNU
Norwegian University of
Science and Technology